

## Electronic Supporting Information

### Supramolecular multivalency effects enhance imine formation in aqueous medium allowing for dynamic modification of enzymatic activity

Ferran Esteve,<sup>\*a</sup> Fidan Rahmatova,<sup>a</sup> Jean-Marie Lehn<sup>\*a</sup>

<sup>a</sup>Laboratoire de Chimie Supramoléculaire, Institut de Science et d'Ingénierie Supramoléculaires (ISIS),  
Université de Strasbourg, 8 allée Gaspard Monge, 67000 Strasbourg, France

#### Table of contents

1. Experimental section.....	S1
2. Main text supporting Figures and Schemes.....	S5
3. Characterization.....	S13
4. MALDI analyses.....	S23
5. DFT cartesian coordinates and energies.....	S29
6. References.....	S42

## 1. Experimental section

### Materials and Methods

All amines, aldehydes and components of buffer solutions were obtained from commercial suppliers and used without further purification. Carbonic anhydrase from bovine erythrocytes (**CA**) was obtained from SigmaAldrich. No unexpected or unusually high safety hazards were encountered.

A Mettler Toledo SevenCompact pH Meter S220 was used to monitor the pH of the solutions, adjusted with either NaOD or DCl solutions as appropriate. All reactions were performed at room temperature, unless otherwise noted. Imination reactions were carried out in 50 mM deuterated phosphate buffer pD 7.2 unless otherwise indicated. The yields and product abundances were determined by relative integration of the signals in the 500 MHz  $^1\text{H}$ -NMR spectra (Bruker Ascend Spectroscopy Advance Neo-500 MHz; 500 MHz for  $^1\text{H}$  and 125 MHz for  $^{13}\text{C}\{^1\text{H}\}$ ). An example of the procedure is illustrated in Fig. S16 and S17 in the characterization section. First, the spectrum was referenced, phased, and the baseline was corrected. Afterwards, the signals of interest were accurately integrated to minimise the residual error, and finally, the numerical values are processed (*e.g.*, integration of the bisimine species is divided by two) for calculating product abundances. The error in integration is of 5%. The identification of the bisimine species was also confirmed by HRMS. All the reactions were analysed after 10 min, 1 h, 24 h, and 48 h to confirm that the equilibrium state was reached. The equilibrium was attained in all reactions after 10 min, except for the condensations between **T** and **A2/A3** in which 1 h was needed. Data analysis was performed using MestReNova (version 14.2.3) and OriginPro (version 9.8.0.200). HRMS-electro-spray ionization (HRMS-ESI) mass spectra were recorded using a ThermoFisher Exactive Plus EMR Orbitrap mass spectrometer. MALDI analyses were performed on a MALDI AUTOFLEX SPEED Bruker using para-Nitroaniline PNA as the matrix. UV-VIS spectroscopy measurements were performed on a JASCO V-670 UV-VIS spectrophotometer. CD spectroscopy measurements were performed on a J-1500 CD spectrophotometer.

### Catalytic experiments and CA inhibition

A method was properly designed for monitoring the kinetic profiles of the assayed hydrolysis reactions. All catalytic transformations were performed in  $\text{D}_2\text{O}$  (pD 7.2, 50 mM phosphate buffer) at 335 K, and the concentrations of **p-NP** were determined using a calibration curve (absorbance at 400 nm). In a typical experiment (inhibition of **CA** using **A8** in a 1:1 molar ratio), 10  $\mu\text{L}$  of a 0.1 mM solution of **CA** were diluted with 970  $\mu\text{L}$  of  $\text{D}_2\text{O}$  (pD = 7.2, PBS, 50 mM). To this solution, 10  $\mu\text{L}$  of a 0.1 mM solution ( $\text{D}_2\text{O}$ , pD = 7.2, PBS, 50 mM) of **A8** were added and the mixture was equilibrated for 10 min. Subsequently, 10  $\mu\text{L}$  of a 10 mM solution of **p-NPA** ( $\text{CH}_3\text{CN}$ ) were added and the kinetic profile for the hydrolysis reaction was monitored over 20 min.

### Titration experiments

The concentration of **CA** was maintained constant during the consecutive additions of **A8**. For the NMR titration, 0.3 mM solution of **CA** in 0.4 mL of  $\text{D}_2\text{O}$  (pD = 7.2, PBS, 50 mM) was treated with increasing amounts of a 1 mL stock solution (pD = 7.2, PBS, 50 mM) of **A8** (10 mM) that also contained 0.3 mM of **CA**. A similar procedure was followed for the CD titration experiment, using

in this case a 0.001 mM solution of **CA** and a 0.1 mM stock solution of **A8** (containing 0.001 mM of **CA**), both in D<sub>2</sub>O (pD = 7.2, PBS, 50 mM).

### DFT calculations

DFT calculations were performed using Gaussian 09 (revision B.01) at the b3lyp level of theory using the 6-31g(d,p) basis set.<sup>1,2</sup> All free energies (kcal/mol) were calculated taking into account the energies of the corresponding reagents and the molecule of water (as its H<sub>3</sub>O<sup>+</sup> ion, considering that the amino components were calculated as their ammonium derivatives) released in the condensation reaction. The DFT models were calculated at room temperature and using water as the solvent (PCM).<sup>3</sup> 3D representations were designed using the Mercury software. It must be noted that the free-energy values are only suitable for comparison between systems, as the energy of the compounds will depend on the protonation degree of each of the species, and thus it might change according to both pK<sub>a</sub> of the corresponding components and the pH of the medium. For all calculations, the highest degree of protonation was considered for the compounds to maximize the effect of possible interactions between charged groups.

### Docking analyses

SwissDock is an open source web server-based molecular docking engine, and it can be accessed at <http://www.swissdock.ch/>. This webserver is developed and maintained by the Swiss Institute of Bioinformatics, Lausanne, Switzerland.<sup>4</sup> The molecular structure of **CA** was download from PDB database (pdb: 1v9e). The molecular structure of **A8** was modeled at the b3lyp level of theory using the 6-31g(d,p) basis set. Both structures were uploaded on the SwissDock web server, and their interaction was elucidated using a blind and accurate docking for screening all possible recognition sites. Binding energies for the different interaction modes were recorded. The top-ranked pose was selected ( $\Delta G = -8.15$  kcal/mol) and it was represented using Chimera 1.16 software (Fig. S10).

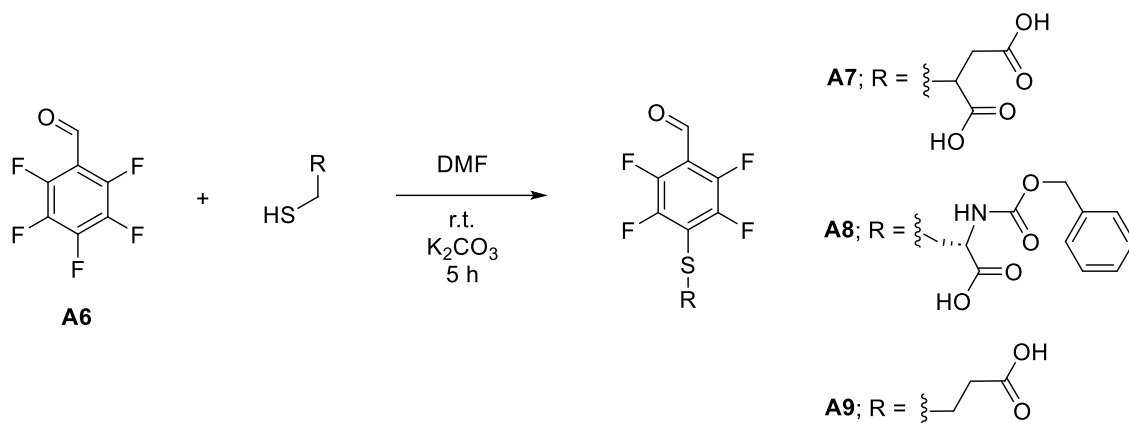
### Synthetic protocols

**Synthesis of A9.** K<sub>2</sub>CO<sub>3</sub> (1.2 eq., 0.67 g, 4.86 mmol) was suspended on dry DMF (10 ml) in an atmosphere of N<sub>2</sub>. 3-thiolpropanoic acid (1 eq., 0.43 g, 0.35 mL, 4.05 mmol) was then dissolved in DMF (10 mL) and added to the reaction suspension. 2,3,4,5,6-Pentafluorobenzaldehyde (**A6**) (1 eq., 0.79 g, 0.5 ml, 4.05 mmol) was introduced to the mixture and stirred for 5 h at 20°C. The solvent was removed in vacuo and acid water (pH 4, 20 ml) was added to the dried solid. The resulting solution was extracted with EtOAc (3x40 mL). The combined organic phases were dried over Na<sub>2</sub>SO<sub>4</sub>, filtered, and evaporated under reduced pressure to yield pure **A6** (449 mg, 1.59 mmol, 39% yield) as a yellow solid. Characterization: m.p.= 103-105 °C. FTIR (ATR): 2899, 2706-2498(bs), 1692, 1636, 1466, 1409, 1279. <sup>1</sup>H-NMR (500 MHz, DMSO-d<sub>6</sub>)  $\delta$  (ppm) 12.42 (s, 1H), 10.16 (s, 1H), 3.24 (t, J = 6.79 Hz, 2H), 2.58 (t, J = 6.79 Hz, 2H). <sup>13</sup>C{<sup>1</sup>H}-NMR (500 MHz, DMSO-d<sub>6</sub>)  $\delta$  (ppm) 184.0, 172.8, 147.4, 145.6, 121.3, 114.8, 35.1, 29.8. HRMS-QTOF(-) calcd for C<sub>10</sub>H<sub>5</sub>F<sub>4</sub>O<sub>3</sub>S: 280.9901, found 280.9890. See Fig. S18-S20 and S27 for characterization.

**Synthesis of A8.** This compound was synthesized following the same procedure as described for **A6** (0.42 g, 0.98 mmol, 21% yield, brownish solid). Characterization: m.p.= 191-192 °C. FTIR (ATR): 3311, 2959, 2802-2408(bs), 1746, 1702, 1635, 1509, 1278, 1212. <sup>1</sup>H-NMR (500 MHz, DMSO-d<sub>6</sub>) δ (ppm) 13.07 (s, 1H), 10.13 (s, 1H), 7.71 (d, J = 8.6 Hz, 1H), 7.37-7.28 (m, 6H), 4.98 (s, 2H), 4.18 (m, 1H), 3.58-3.51 (m, 2H). <sup>13</sup>C{<sup>1</sup>H}-NMR (500 MHz, DMSO-d<sub>6</sub>) δ (ppm) 183.9, 171.8, 156.3, 147.5, 145.4, 136.7, 128.8, 128.4, 128.0, 121.2, 114.8, 66.1, 54.9, 35.2. HRMS-QTOF(-) calcd for C<sub>18</sub>H<sub>12</sub>F<sub>4</sub>O<sub>5</sub>SN: 430.0378, found 430.0367. See Fig. S21-S23 and S28 for characterization.

**Synthesis of A7.** This compound was synthesized following the same procedure as described for **A6** (0.88 g, 2.703 mmol, 53% yield, yellow solid). Characterization: m.p.= 157-158 °C. FTIR (ATR): 2873, 2702-2525(bs), 1698, 1635, 1465, 1420, 1278. <sup>1</sup>H-NMR (500 MHz, DMSO-d<sub>6</sub>) δ (ppm) 12.88 (bs, 2H), 10.16 (s, 1H), 4.10 (dd, J = 7.78, 6.56 Hz, 1H), 2.78 – 2.71 (m, 2H). <sup>13</sup>C{<sup>1</sup>H}-NMR (500 MHz, DMSO-d<sub>6</sub>) δ (ppm) 183.9, 171.7, 171.3, 148.6, 146.6, 117.9, 116.5, 45.3, 36.6. HRMS-QTOF(-) calcd for C<sub>11</sub>H<sub>5</sub>F<sub>4</sub>O<sub>5</sub>S: 324.9799, found 324.9788. See Fig. S24-S26 and S29 for characterization.

## 2. Main text supporting Figures, Schemes and Tables



**Scheme S1.** Synthetic route for the herein proposed water-soluble reactive aldehydes, viz. **A7**, **A8**, and **A9**.

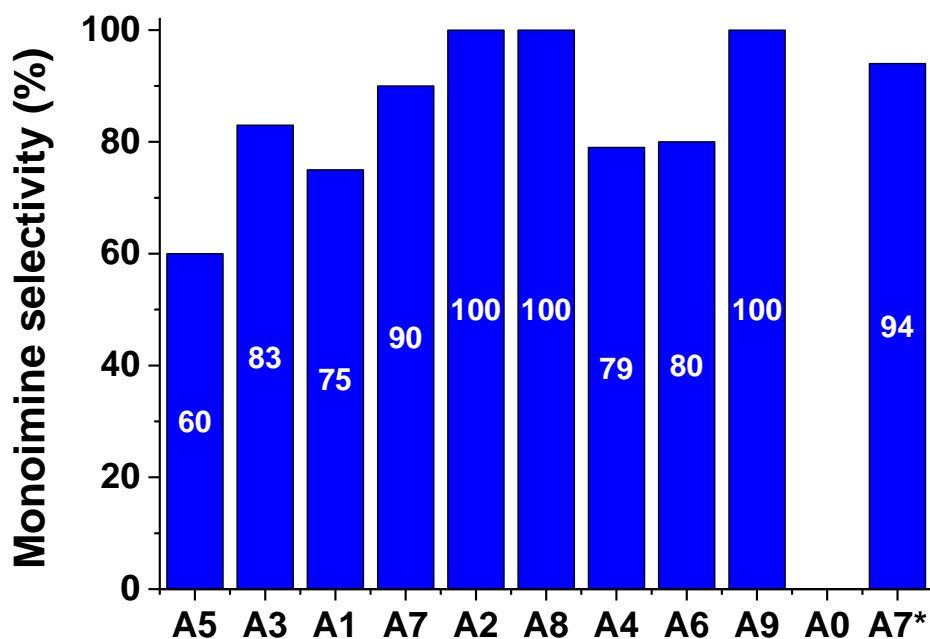


**Fig. S1.** Monoimine selectivity (over the bisimino species detected) attained in the reaction between **T** and the different aldehydes assayed. Selectivity calculated according to the formula:  $S=100 \cdot I_{\text{monoimine}} / (I_{\text{monoimine}} + [I_{\text{bisimine}}/2])$ . Integrations (*I*) determined using  $^1\text{H}$  NMR spectroscopy (500 MHz, 295 K). Reaction conditions:  $\text{D}_2\text{O}$  (pD = 7.2, phosphate buffer 50 mM), 295 K,  $[\text{AX}] = [\text{T}] = 5$  mM. A7\*:  $[\text{A7}] = 5$  mM,  $[\text{T}] = 50$  mM. Results have been sorted following the order of Fig. 2 in the main text for clarity.

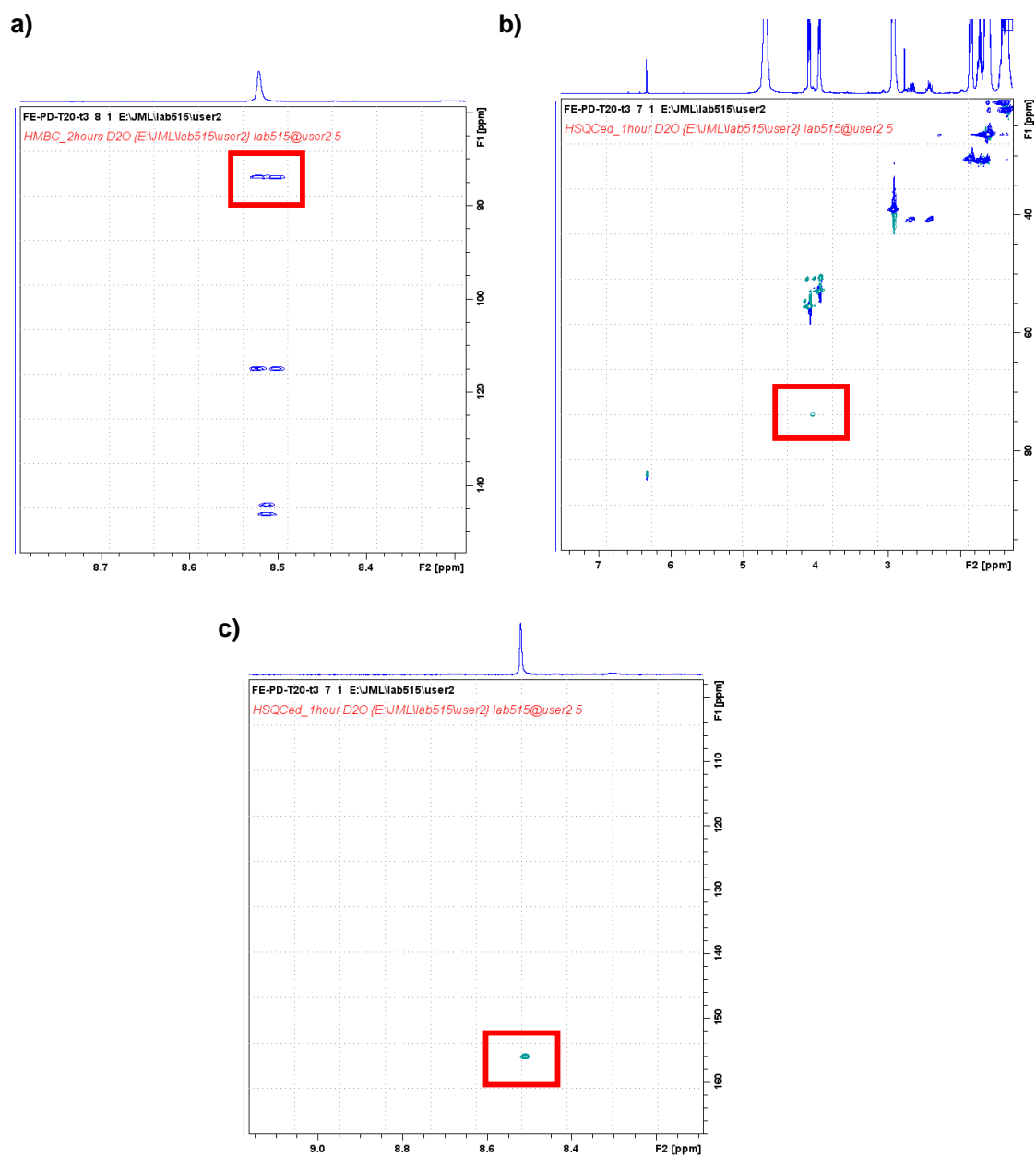


**Fig. S2.** 2D NMR analyses (500 MHz, 295 K,  $\text{D}_2\text{O}$ ,  $\text{pD} = 7.2$ ) for the reaction between **A7** and **KOMe** after 1 h. a) Partial HMBC showing the correlation between CH imine (8.52 ppm) and the  $^{13}\text{C}$  signal at 73.7 assigned to the stereogenic carbon of **KOMe** (right next to the  $\text{N}\alpha$ ). b) and c) show the partial edited HSQC in which the CH groups are coloured in green and the  $\text{CH}_2$  in blue. The most relevant peaks have been highlighted with a red square for clarity.

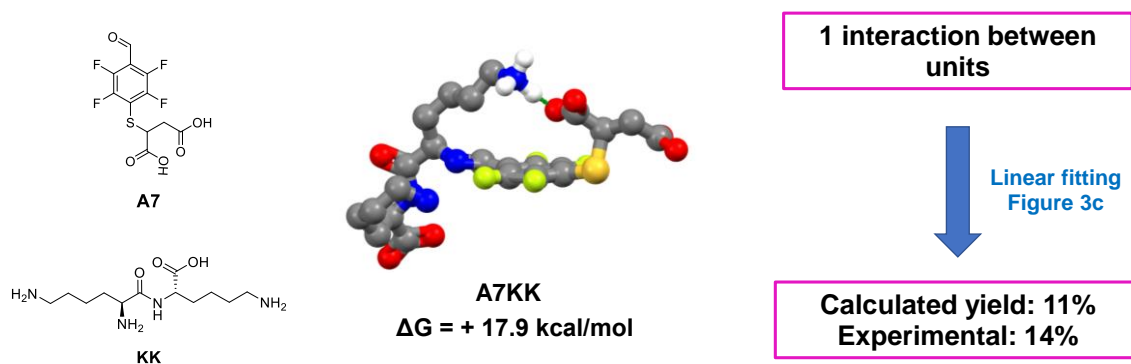


**Fig. S3.** DFT (b3lyp, 6-31g(d,p)) calculated lowest in energy conformation for imine **A7KK**. The supramolecular interaction (hydrogen bond/electrostatic) has been highlighted with a discontinuous green line. Non-essential hydrogen atoms have been omitted for clarity.

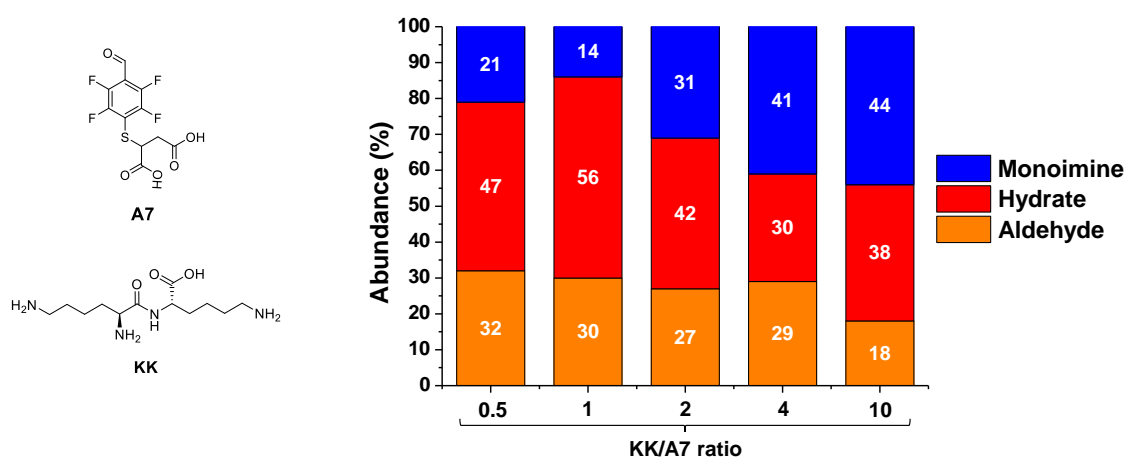


**Fig. S4.** Results for the **A7:KK** molar ratio assays. Component abundance (%) as calculated from  $^1\text{H}$  NMR spectra (500 MHz, 295 K,  $\text{D}_2\text{O}$ ). Reaction conditions:  $\text{D}_2\text{O}$  (pD = 7.2, phosphate buffer 50 mM), 295 K, 1 h, 5 mM concentration for the limiting reagent.

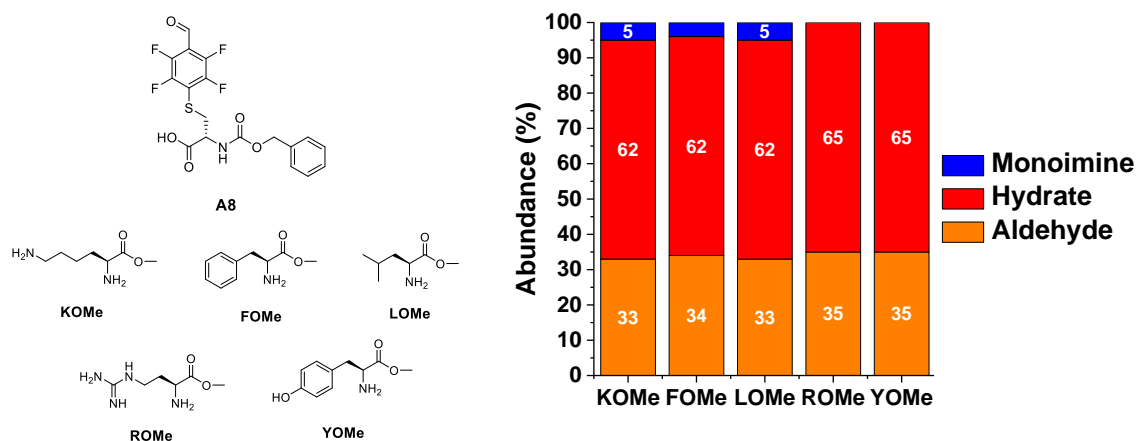


**Fig. S5.** Chemical structures of the aldehyde **A8** and the different methyl ester derivatives of selected amino acids. Component abundances (%) as calculated from  $^1\text{H}$  NMR spectra (500 MHz, 295 K,  $\text{D}_2\text{O}$ ). Reaction conditions:  $\text{D}_2\text{O}$  (pD = 7.2, phosphate buffer 50 mM), 295 K, 1h,  $[\text{A8}] = [\text{XOMe}] = 5$  mM.

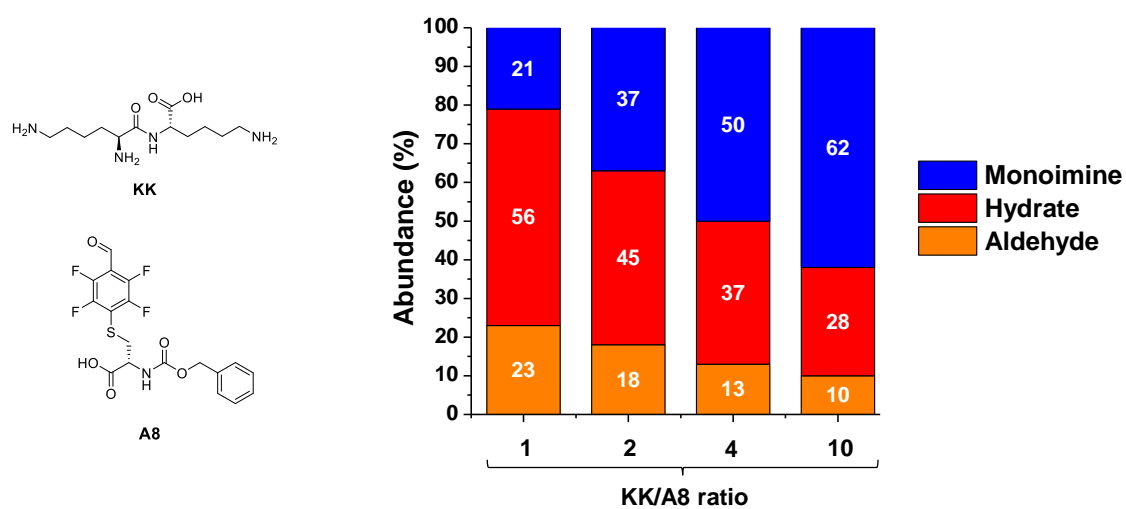


**Fig. S6.** Results for the **A8:KK** molar ratio assays. Component abundance (%) as calculated from  $^1\text{H}$  NMR spectra (500 MHz, 295 K,  $\text{D}_2\text{O}$ ). Reaction conditions:  $\text{D}_2\text{O}$  (pD = 7.2, phosphate buffer 50 mM), 295 K, 1 h, 5 mM concentration for the limiting reagent.



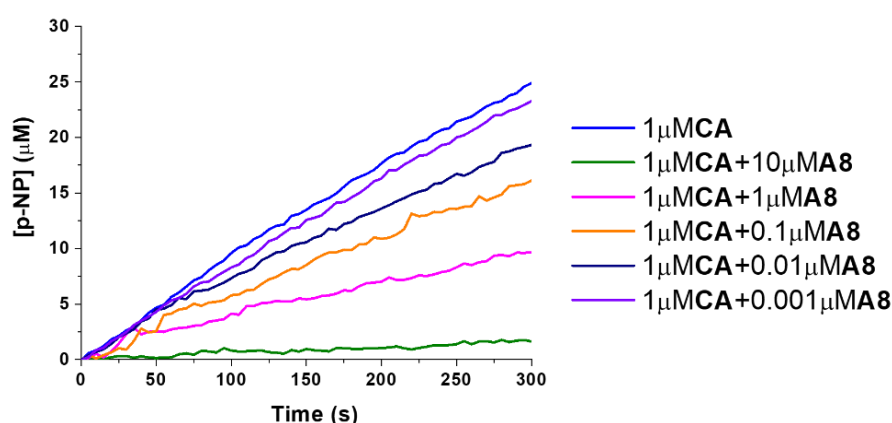


**Fig. S7.** UV monitoring (linear range, 0-300 min) of the hydrolysis of **p-NPA** in the presence of **CA** and different equivalents of **A8**. Reaction conditions:  $D_2O$  (pD = 7.2), 335 K.

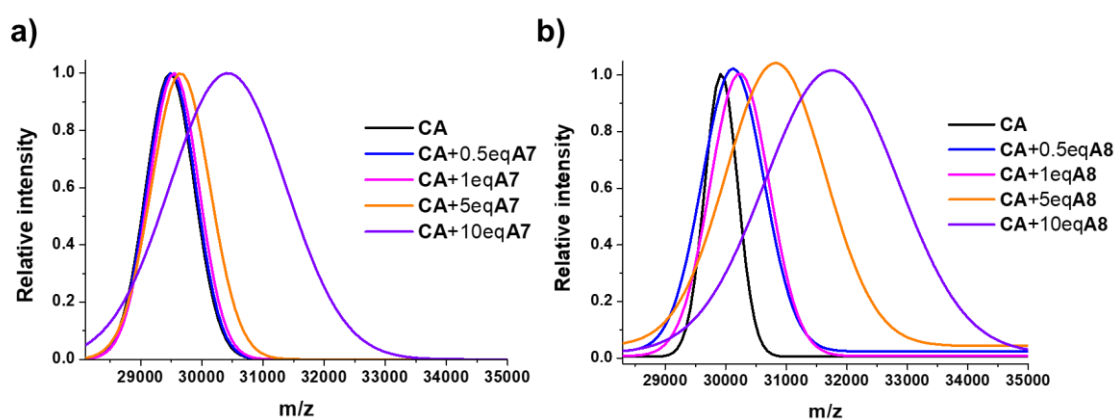


**Fig. S8.** MALDI analyses (PNA matrix,  $D_2O$ , pD 7.2 phosphate buffer) for **CA** (0.1 mM) with increasing amounts of **A7** (a) and **A8** (b). The peaks were fitted to a Gaussian distribution and the mean  $m/z$  was used for quantification of the bioconjugation efficiency; see Fig. 6e. See also Fig. SX-SY for full  $m/z$  scale MALDI analyses. The dispersity of the bioconjugation was estimated using the standard deviation of the fitting: (a) **CA** ( $\sigma = 395.4$ ), **CA+0.5eqA7** ( $\sigma = 398.7$ ), **CA+1eqA7** ( $\sigma = 407.3$ ), **CA+5eqA7** ( $\sigma = 477.9$ ), **CA+10eqA7** ( $\sigma = 950.3$ ); (b) **CA** ( $\sigma = 271.9$ ), **CA+0.5eqA8** ( $\sigma = 511.8$ ), **CA+1eqA8** ( $\sigma = 488.3$ ), **CA+5eqA8** ( $\sigma = 823.6$ ), **CA+10eqA8** ( $\sigma = 1104.1$ ).

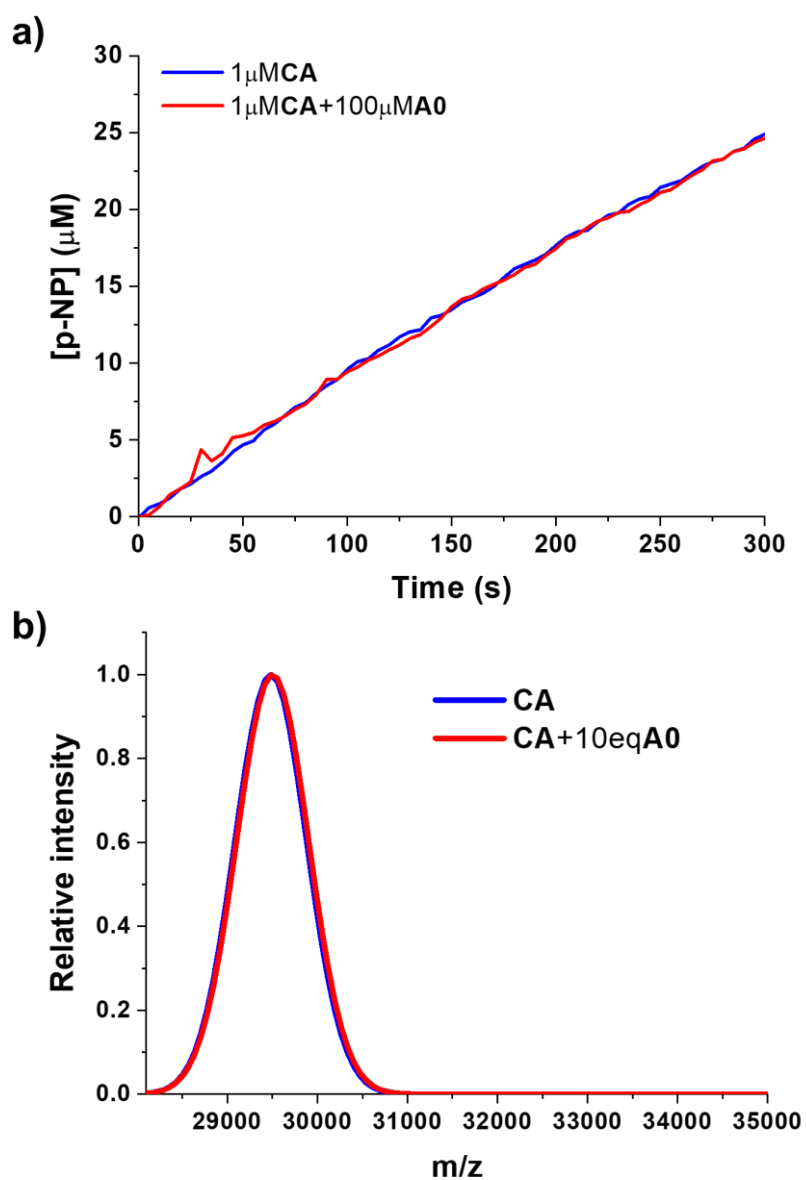


**Fig. S9.** (a) UV monitoring (linear range, 0-300 min) of the hydrolysis of **p-NPA** in the presence of **CA** and **A0** (100eq.). Reaction conditions:  $\text{D}_2\text{O}$  (pD = 7.2), 335 K. (b) MALDI analyses (PNA matrix,  $\text{D}_2\text{O}$ , pD 7.2 phosphate buffer) for **CA** (0.1 mM) in the presence of **A0** (10eq.). The peaks were fitted to a Gaussian distribution.

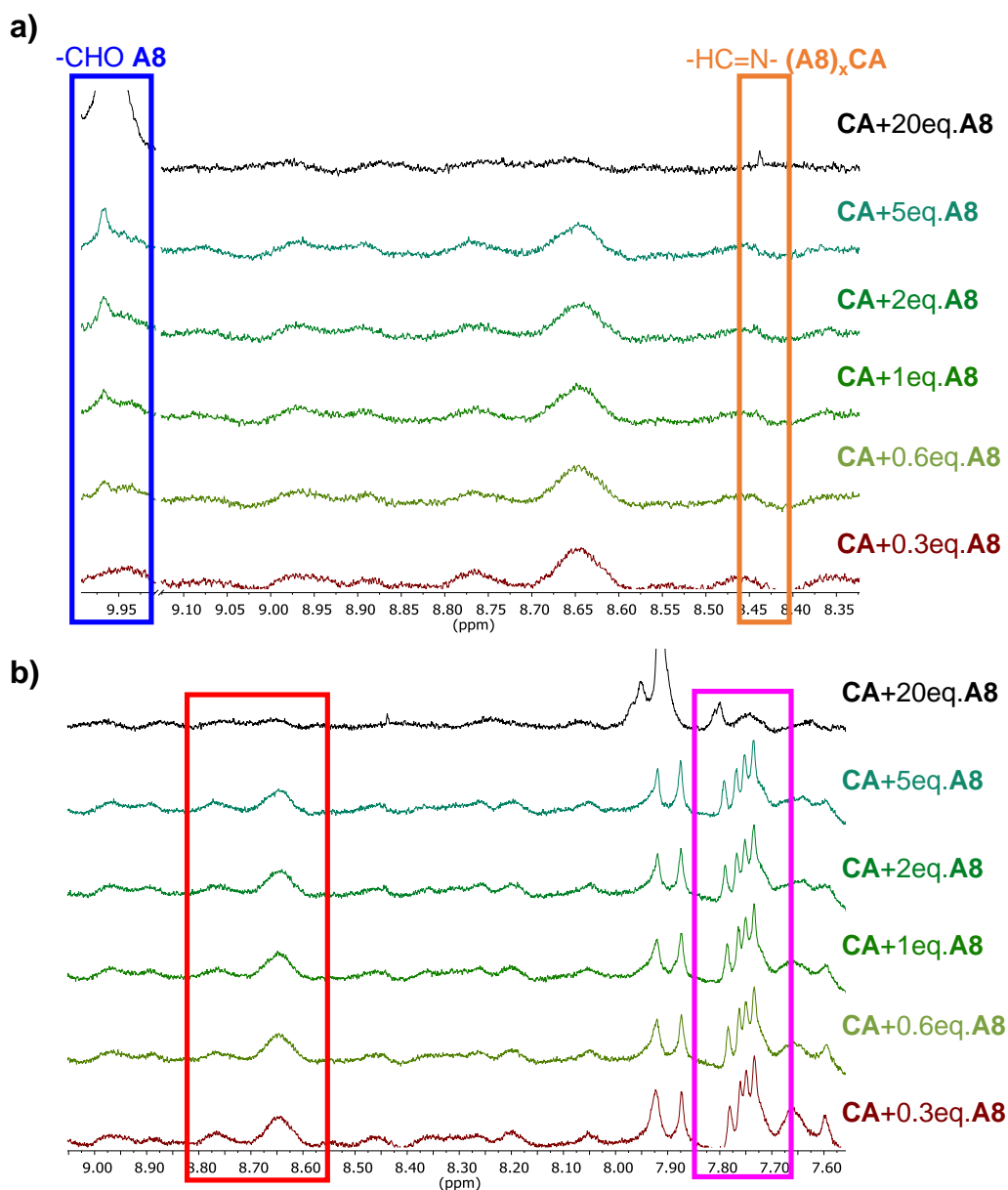


**Fig. S10.** Partial  $^1\text{H}$  NMR (500 MHz,  $\text{D}_2\text{O}$ , pH = 7.2, 295 K) spectra for the titration experiment between CA (0.25 mM) and A8. a) Signals corresponding to aldehyde -CHO and imine -HC=N- have been highlighted with blue and orange rectangles, respectively. b) Regions of the spectra that experience a shift in the presence of A8 have been highlighted with a pink rectangle. On the other hand, some regions of the spectra that do not experience such shifts in the presence of A8 have been highlighted with a red rectangle.

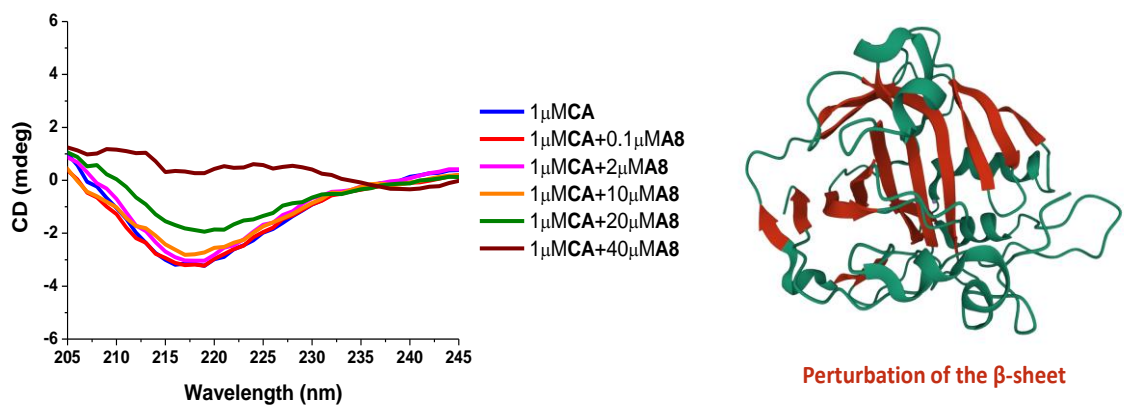


**Fig. S11.** Left: CD spectra ( $D_2O$ ,  $pD = 7.2$ , phosphate buffer, 295 K) for the titration experiment between **CA** and **A8**. Right: 3D-structure of native **CA** from bovine erythrocytes (pdb: 1v9e). The backbone of the protein is coloured green and the  $\beta$ -sheet-like structures are highlighted in orange.

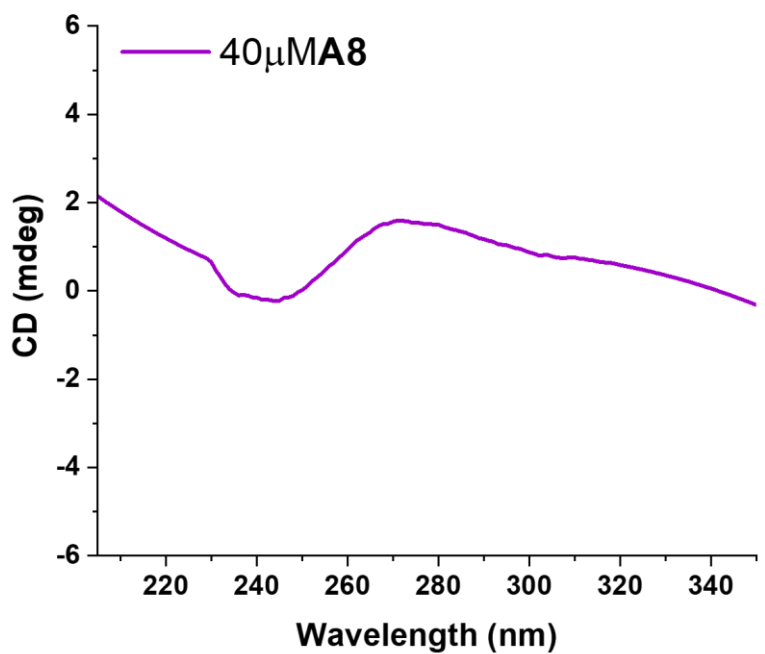


**Fig. S12.** CD spectrum ( $D_2O$ ,  $pD = 7.2$ , phosphate buffer, 295 K) of a 40  $\mu M$  solution in **A8**.

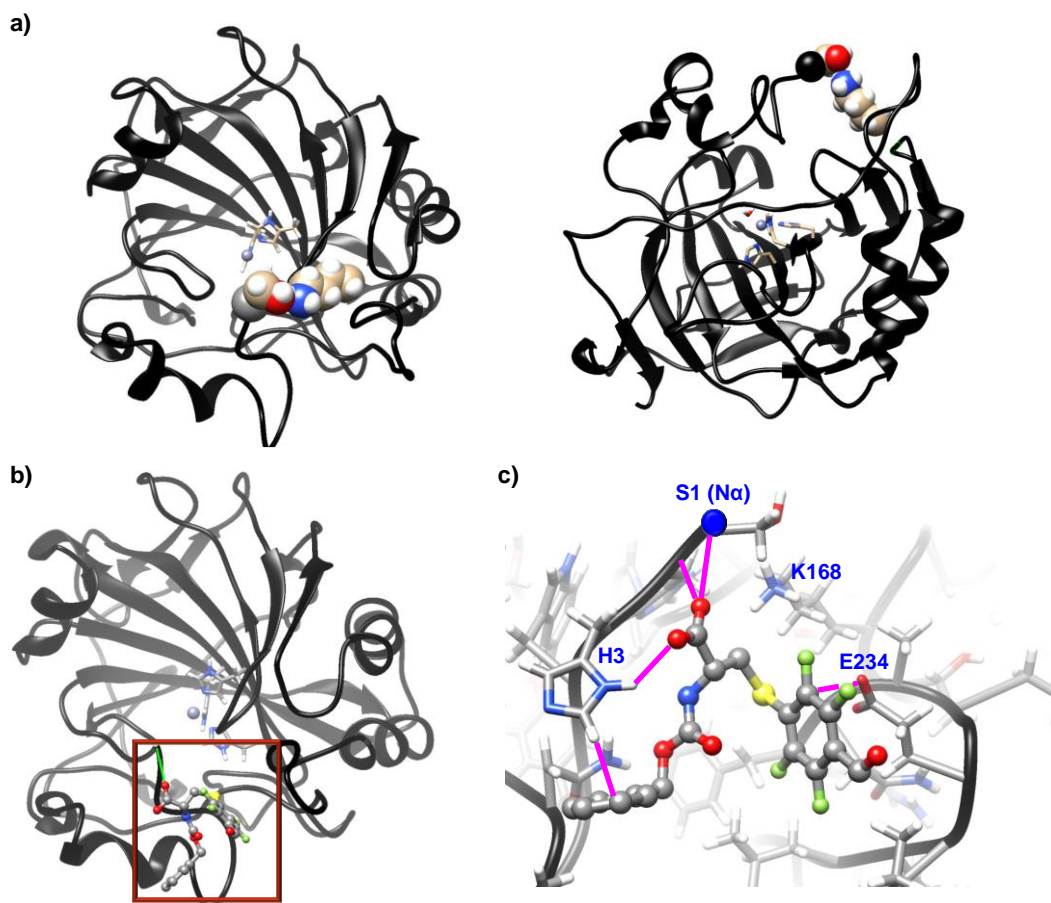


**Fig. S13.** a) Top (left) and side views (right) of **CA** (pdb: 1v9e). The backbone has been represented in black. The active site (in the centre of the conical cavity defined by  $\beta$ -sheets) has been highlighted in capped sticks ( $\text{Zn}^{2+}$  ion represented with the spacefill model in grey). The Ser1 and K168 residues in the entrance of the cavity are highlighted using the spacefill model. b) Best docked pose for the **A8-CA** supramolecular adduct obtained using SwissDock. The region where **A8** is located has been highlighted with a dark red square. Binding free-energy:  $-8.15$  kcal/mol. c) Zoomed-in region for the lowest in energy conformation obtained in the docking experiments. Supramolecular forces have been highlighted with pink lines. Compound **A8** has been represented using the ball and sticks model. All the representation were created using Chimera 1.16 software.

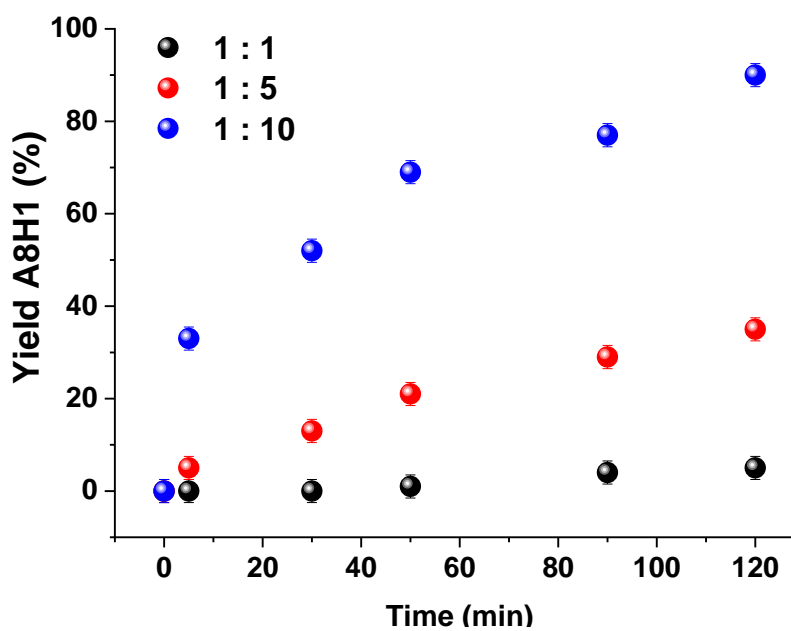


**Fig. S14.** Kinetic profiles for the reaction between **H1** and **A8**, as determined by  $^1\text{H}$  NMR spectroscopy (500 MHz, 295 K,  $\text{D}_2\text{O}$ ,  $\text{pD} = 7.2$ ). Concentrations: 5 mM each (black); 5 mM **A8** + 25 mM **H1** (red); 5 mM **A8** + 50 mM **H1** (blue). Error bars correspond to 5%.

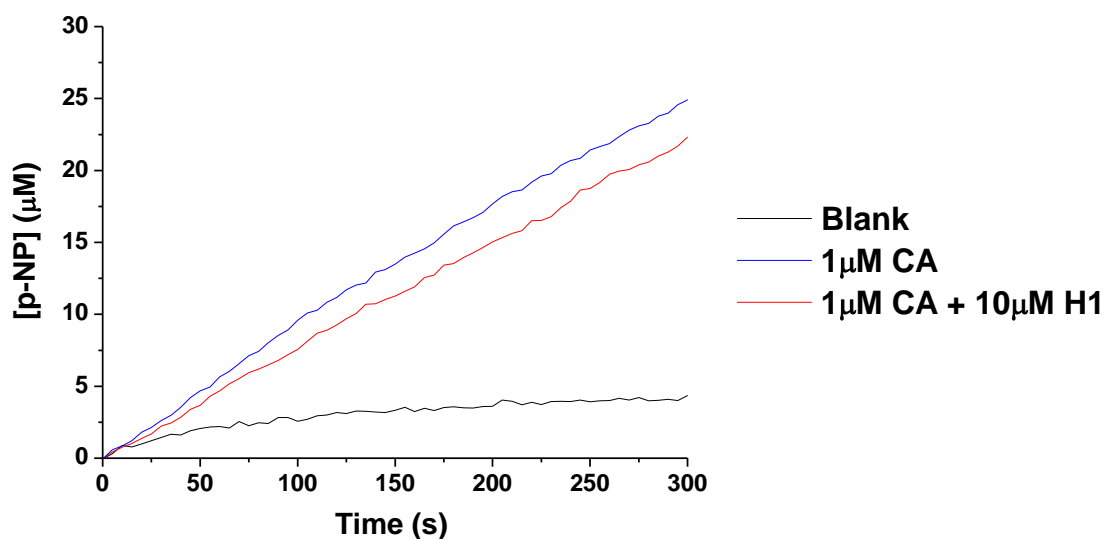


**Fig. S15.** UV monitoring (linear range, 0-300 min) for the hydrolysis of **p-NPA** in the presence of **CA**, and a **CA** : **H1** (1 : 10) mixture. Reaction conditions:  $\text{D}_2\text{O}$  ( $\text{pD} = 7.2$ ), 335 K. The blank has also been added for comparison.

### 3. Characterization

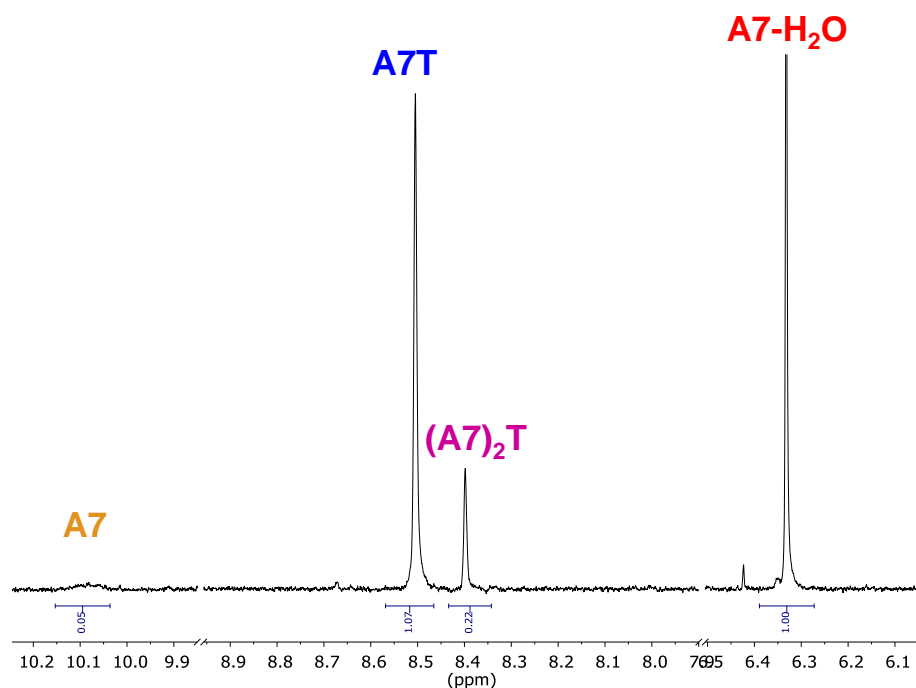


**Fig. S16.** Selected example for the product abundance quantification using <sup>1</sup>H-NMR spectrum (500 MHz, D<sub>2</sub>O + phosphate buffer 50mM, pD 7.2, 295 K). The crude corresponds to the condensation reaction between **A7** and **T** (5 mM each) after 10 mins of equilibration. It must be noted that the integration of the **(A7)<sub>2</sub>T** imine CH signal (8.4 ppm) was divided by two for the quantification of this species since there are two equivalent imine protons per molecule.

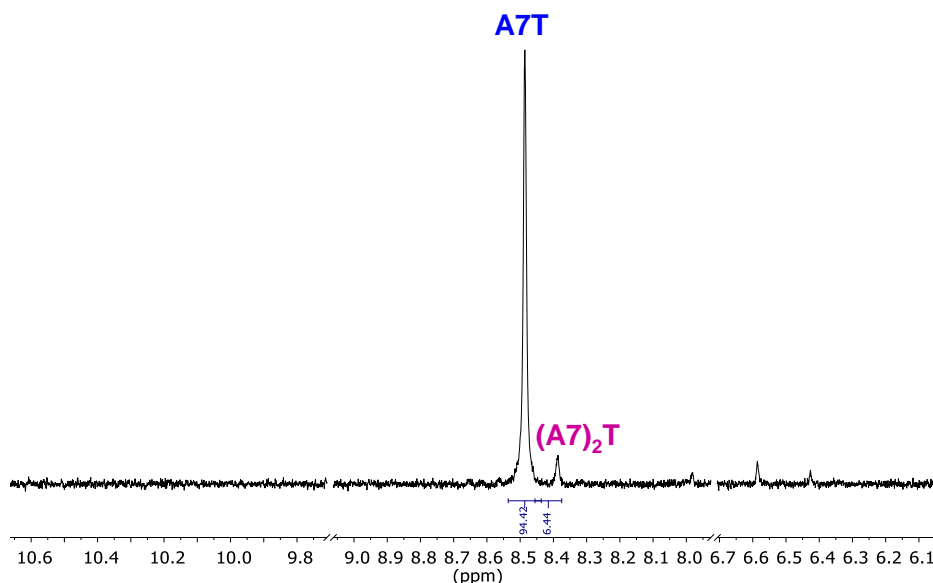


**Fig. S17.** Selected example for the product abundance quantification using <sup>1</sup>H-NMR spectrum (500 MHz, D<sub>2</sub>O + phosphate buffer 50mM, pD 7.2, 295 K). The crude corresponds to the condensation reaction between **A7** and **T** (5 mM **A7** and 50 mM **T**) after 10 mins of equilibration. It must be noted that the integration of the **(A7)<sub>2</sub>T** imine CH signal (8.4 ppm) was divided by two for the quantification of this species since there are two equivalent imine protons per molecule.

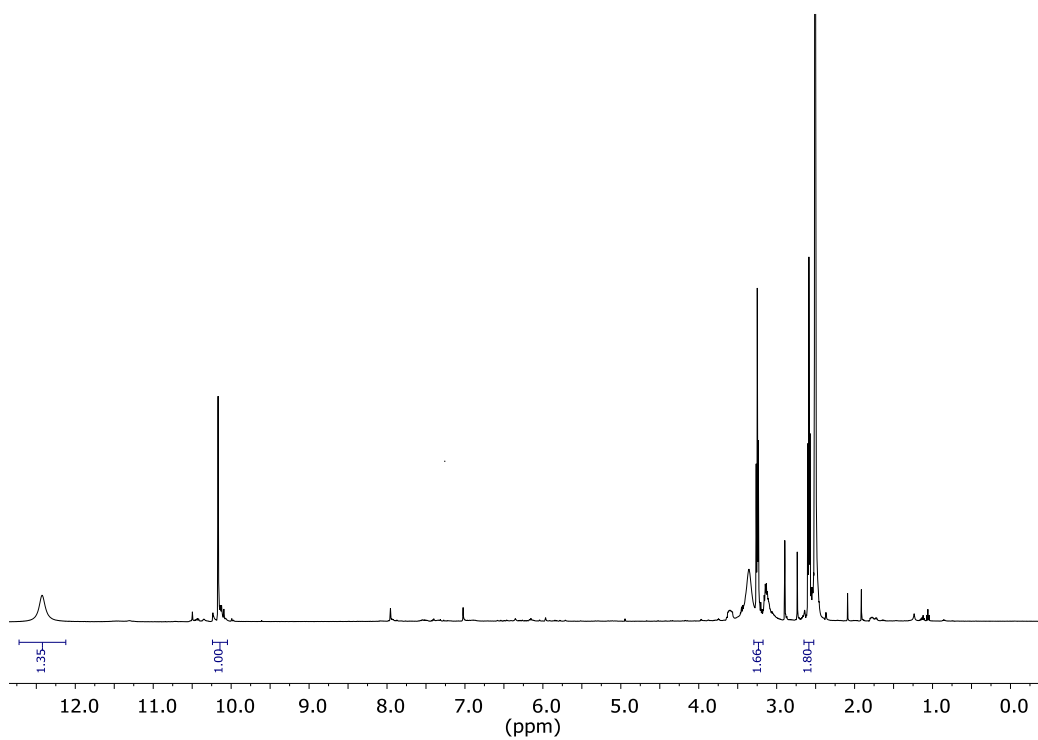


Fig. S18.  $^1\text{H-NMR}$  spectrum (500 MHz, DMSO- $d_6$ , 295 K) of A9.

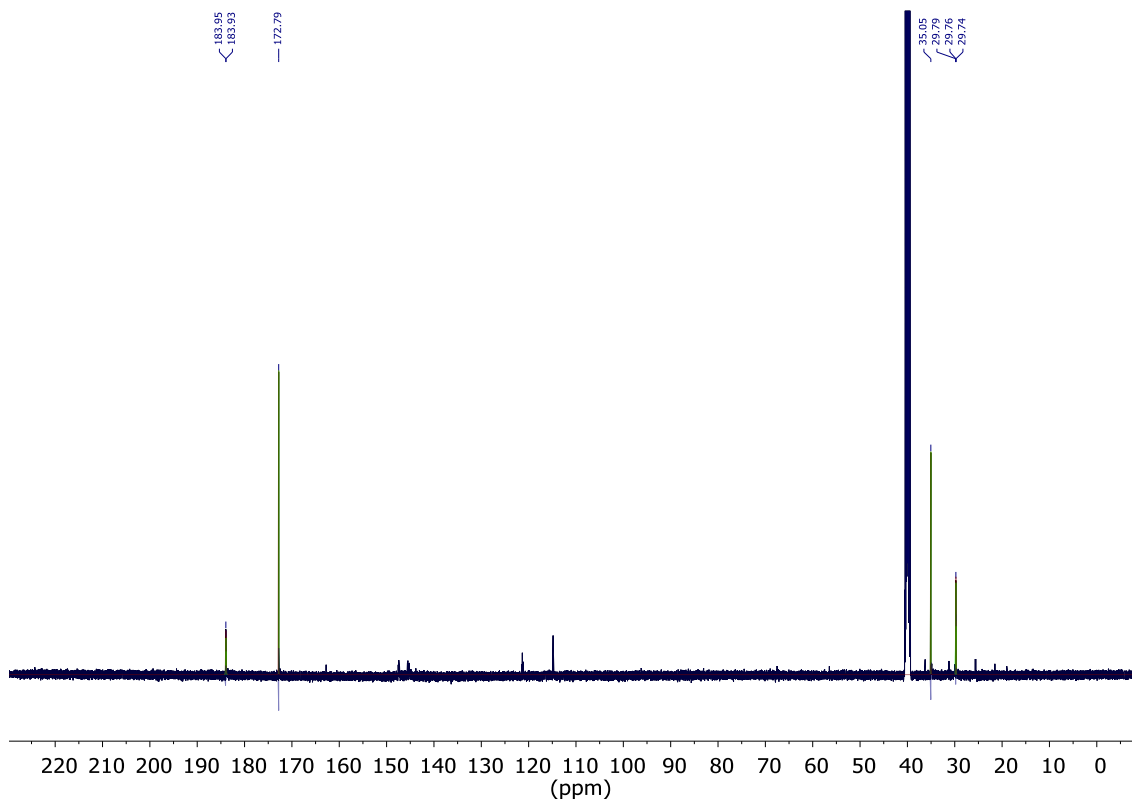
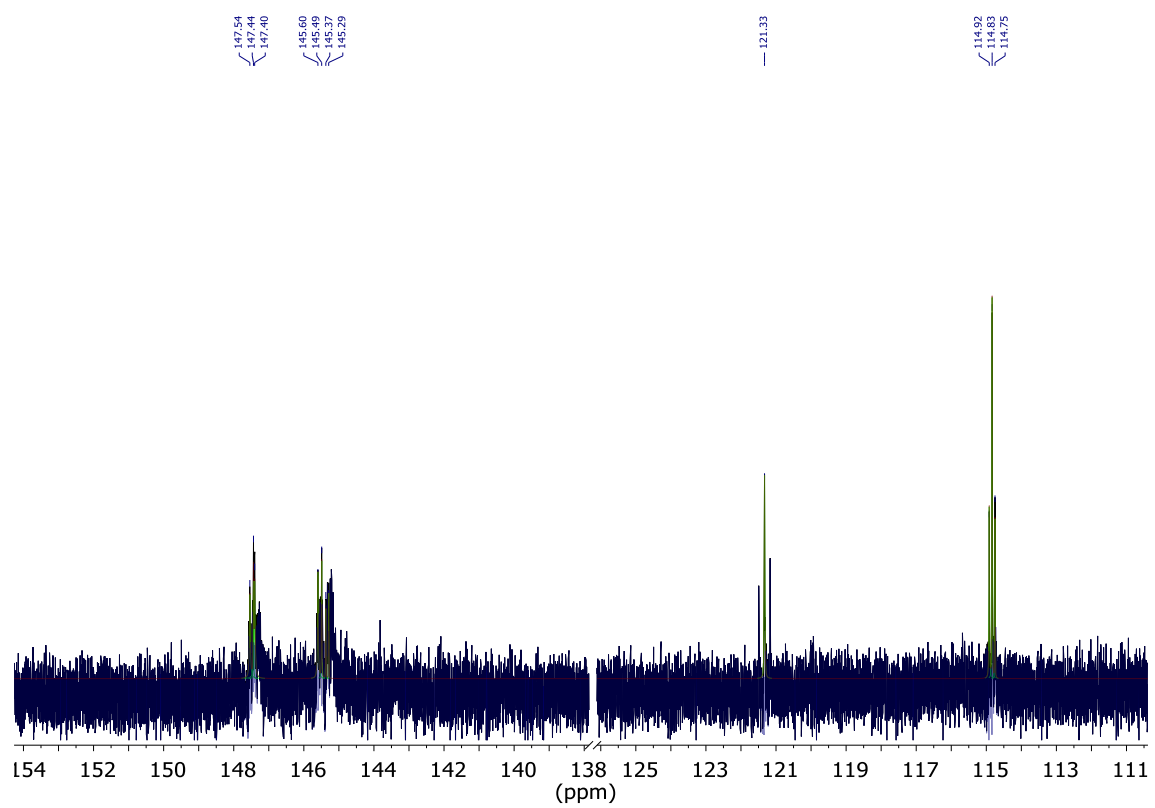


Fig. S19.  $^{13}\text{C}\{^1\text{H}\}$ -NMR spectrum (125 MHz, DMSO- $d_6$ , 295 K) of A9.





**Fig. S20.** Partial  $^{13}\text{C}\{^1\text{H}\}$ -NMR spectrum (125 MHz,  $\text{DMSO-d}_6$ , 295 K) of **A9**.

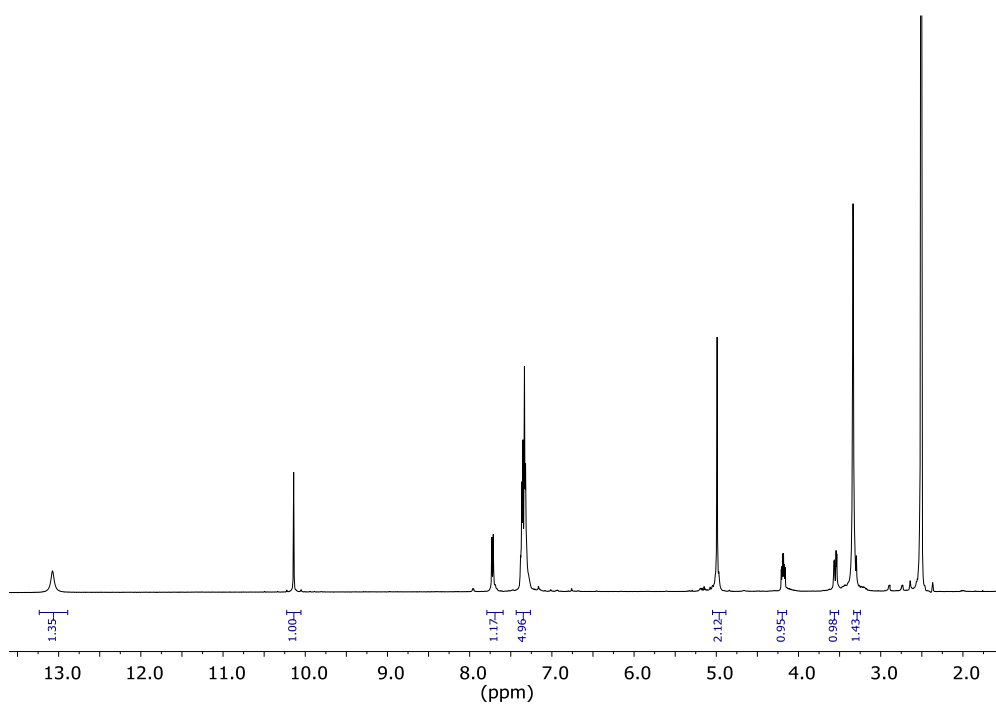


Fig. S21. <sup>1</sup>H-NMR spectrum (500 MHz, DMSO-d<sub>6</sub>, 295 K) of A8.

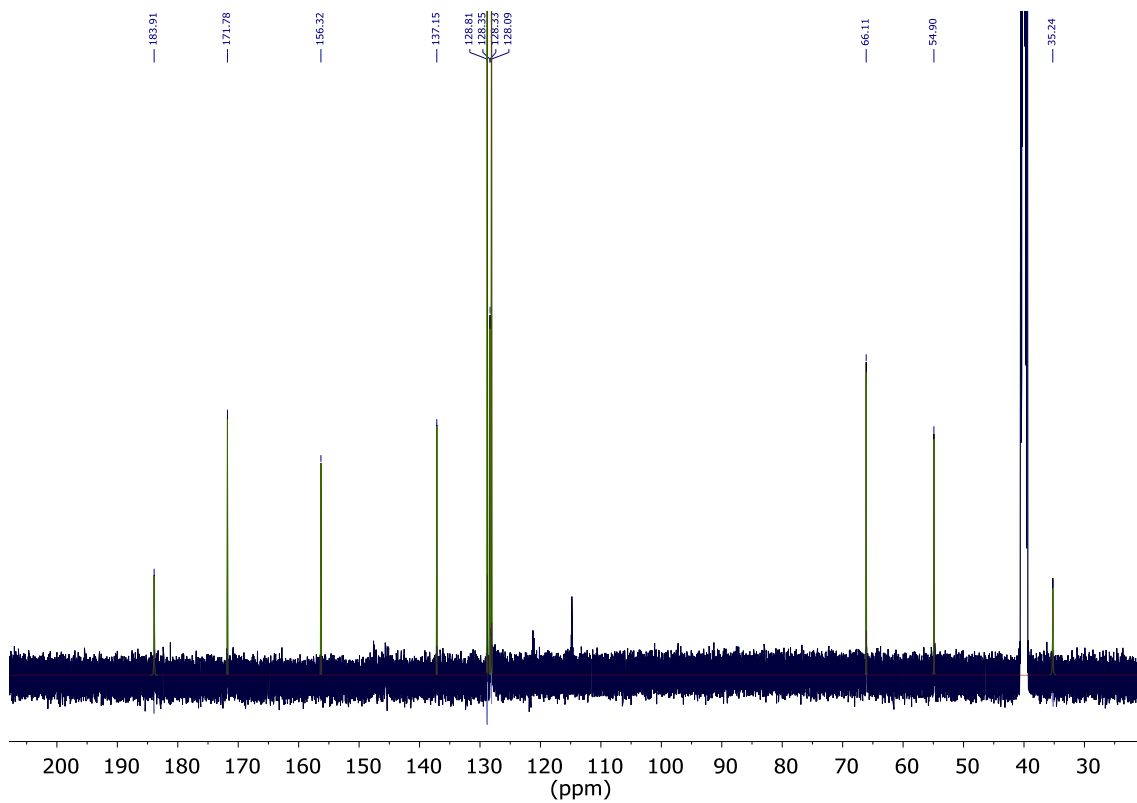


Fig. S22. <sup>13</sup>C{<sup>1</sup>H}-NMR spectrum (125 MHz, DMSO-d<sub>6</sub>, 295 K) of A8.

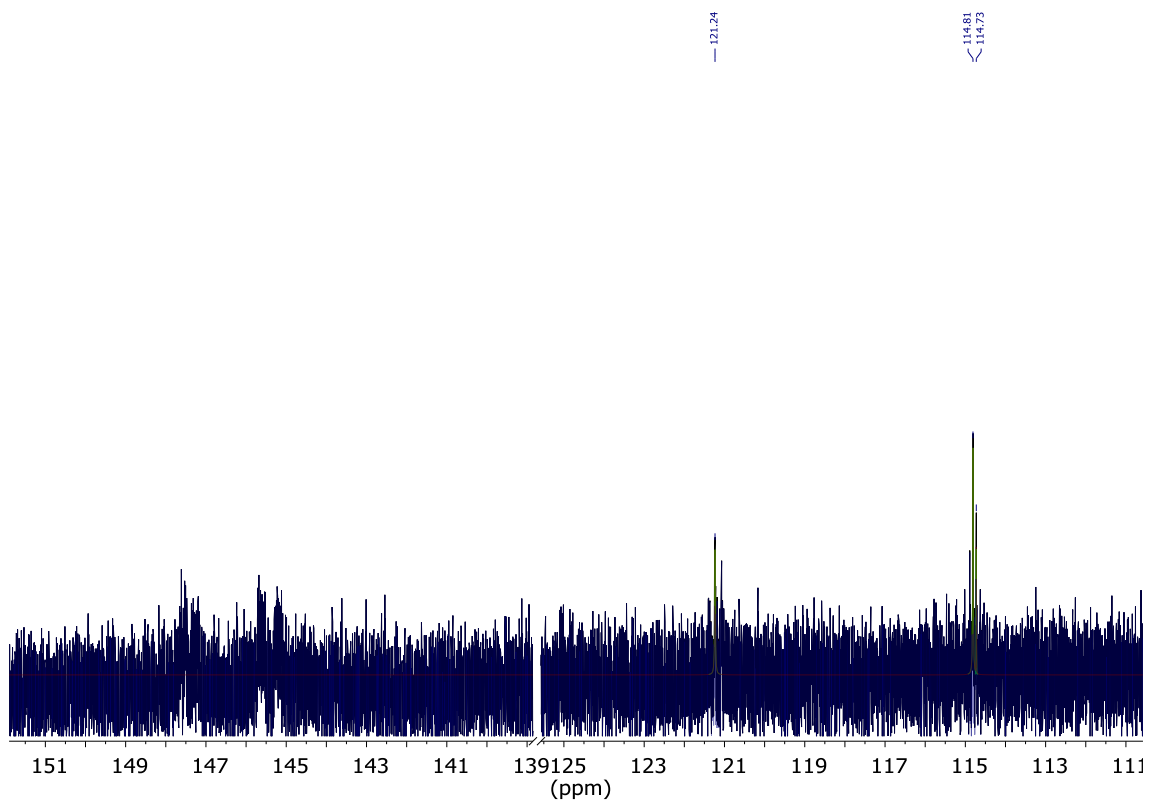


Fig. S23. Partial  $^{13}\text{C}\{^1\text{H}\}$ -NMR spectrum (125 MHz, DMSO- $d_6$ , 295 K) of **A8**.

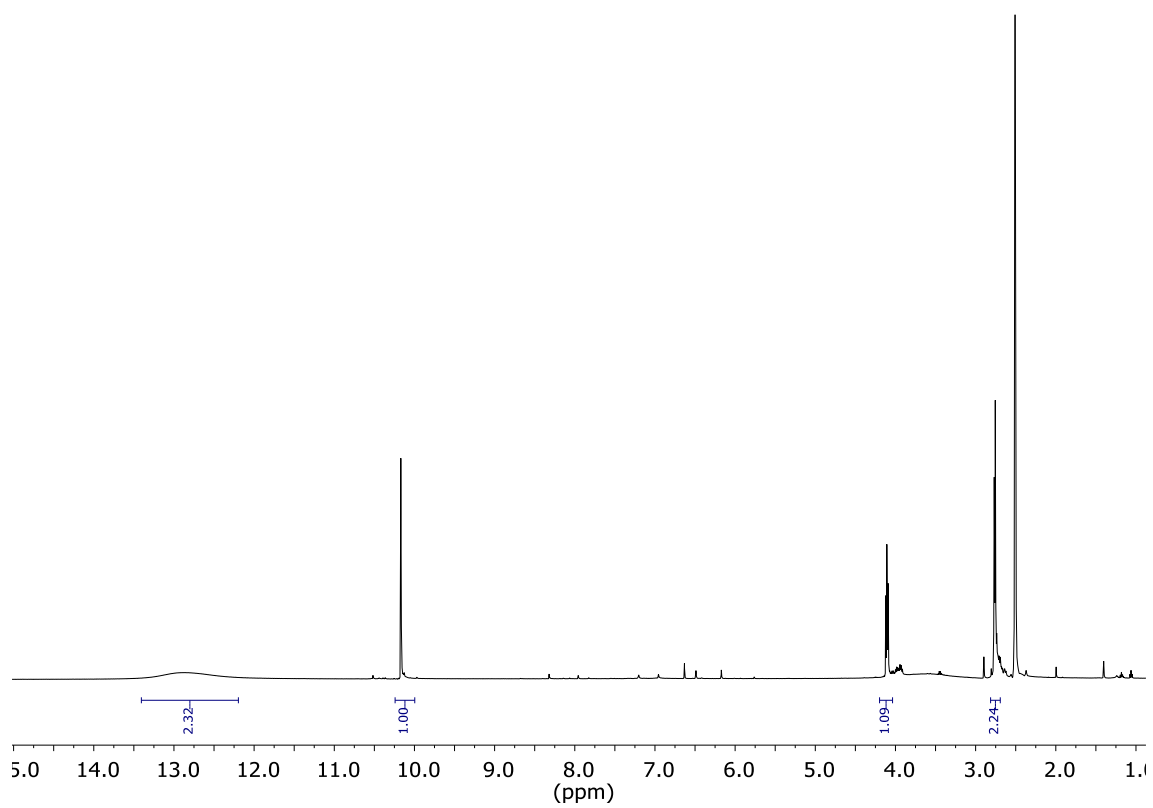


Fig. S24.  $^1\text{H}$ -NMR spectrum (500 MHz, DMSO- $d_6$ , 295 K) of **A7**.

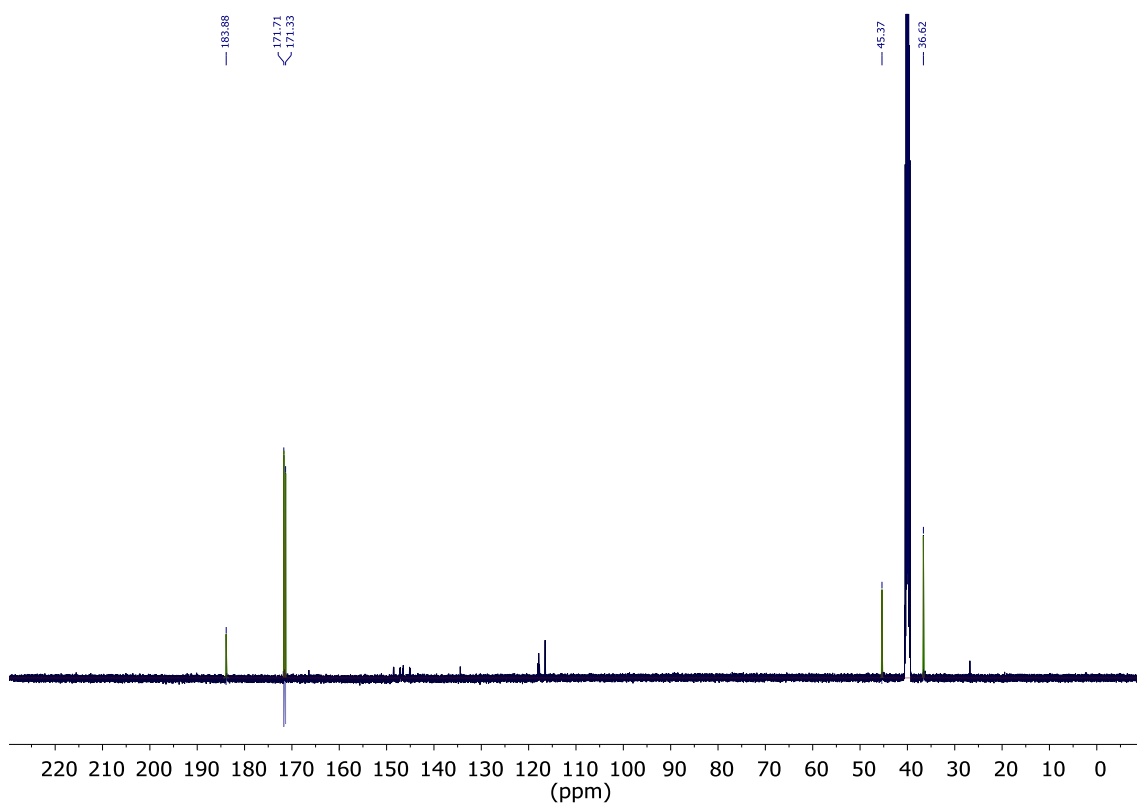


Fig. S25.  $^{13}\text{C}\{^1\text{H}\}$ -NMR spectrum (125 MHz, DMSO- $d_6$ , 295 K) of A7.

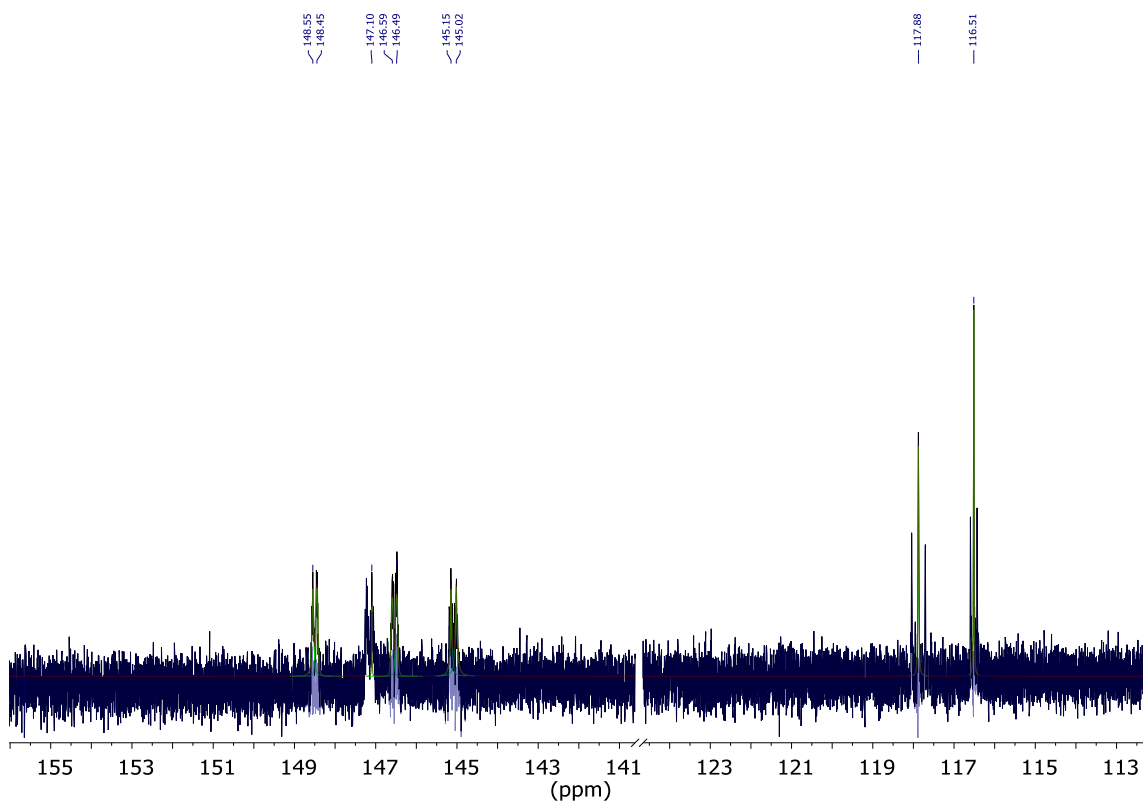


Fig. S26. Partial  $^{13}\text{C}\{^1\text{H}\}$ -NMR spectrum (125 MHz, DMSO- $d_6$ , 295 K) of A7.

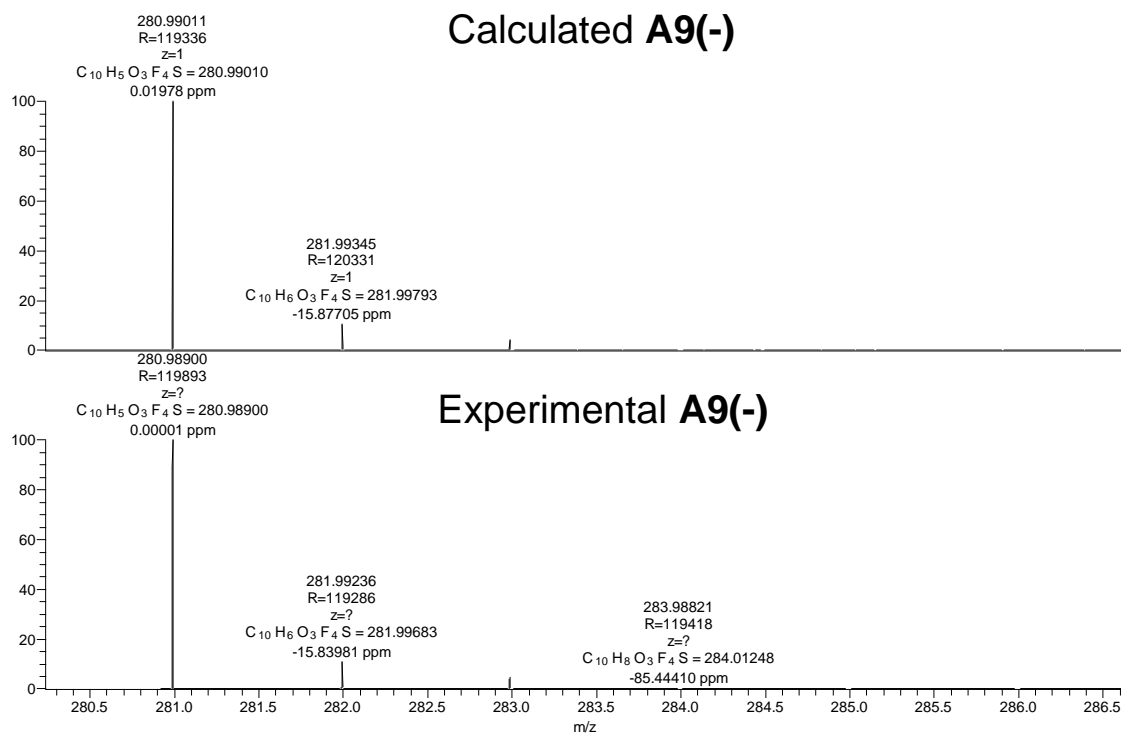


Fig. S27. HRMS-QTOF(-) spectrum (MeOH) of A9.

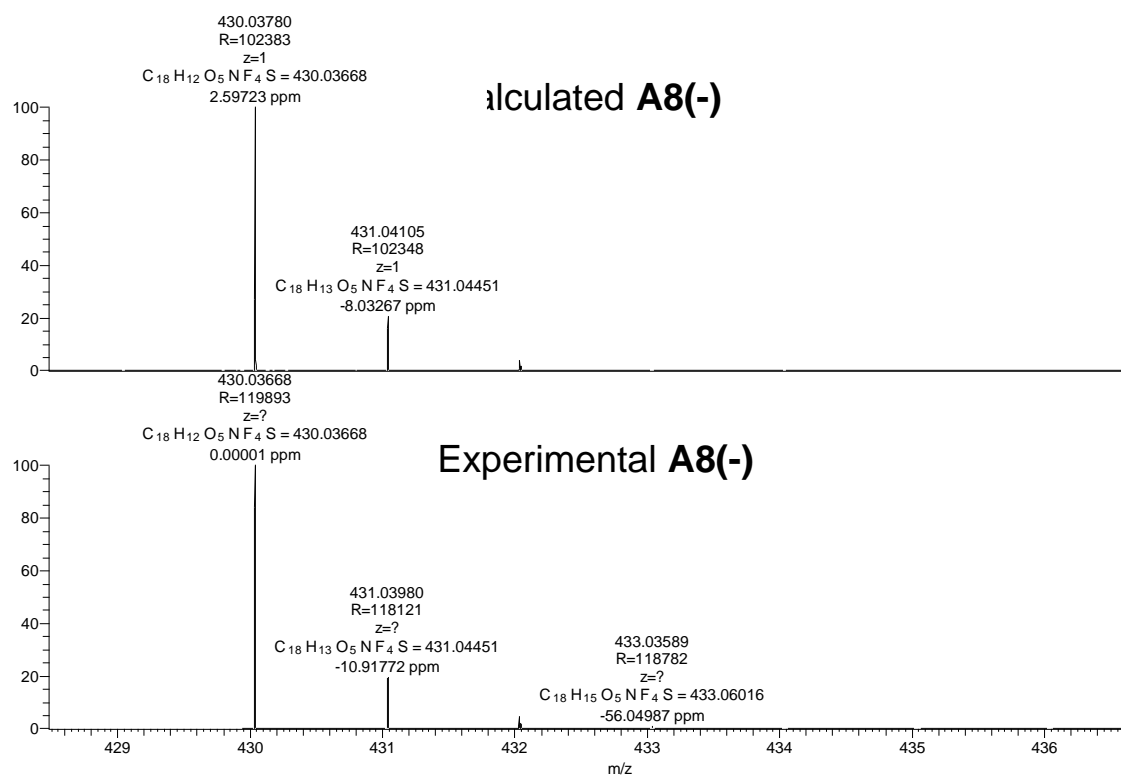


Fig. S28. HRMS-QTOF(-) spectrum (MeOH) of A8.

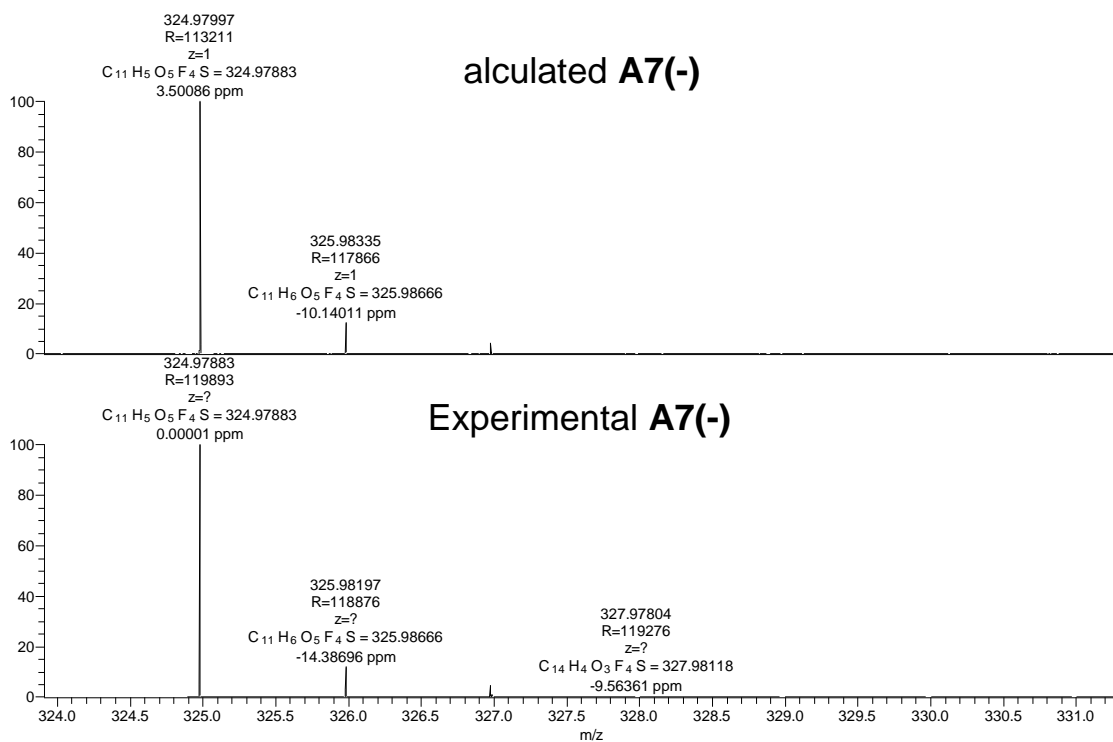
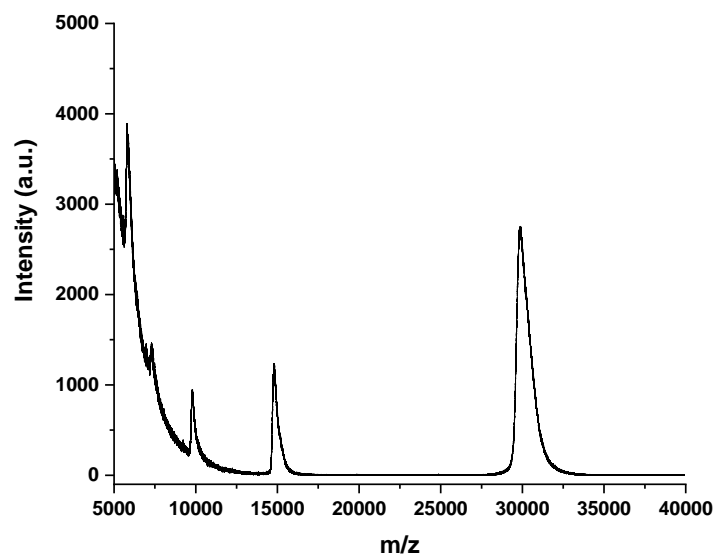
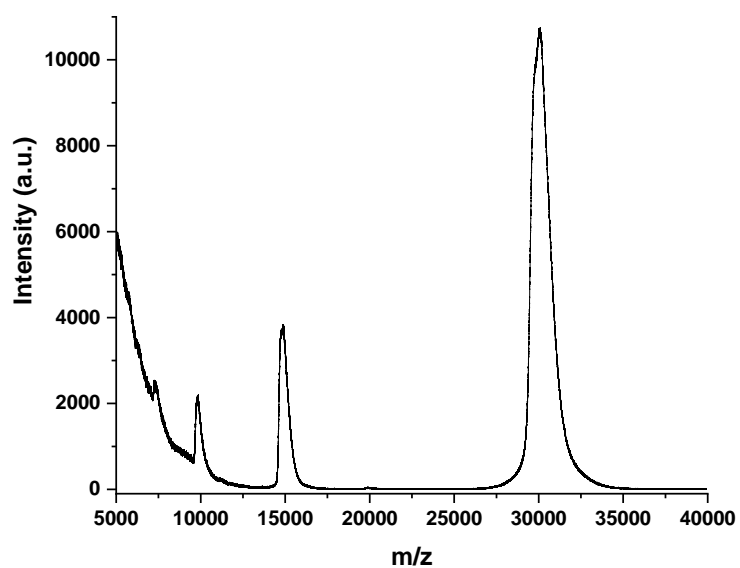


Fig. S29. HRMS-QTOF(-) spectrum (MeOH) of A7.

#### 4. MALDI analyses



**Fig. S30.** MALDI analysis (PNA matrix, D<sub>2</sub>O, pD 7.2 phosphate buffer) of **CA** (0.1 mM) in the absence of **A8**.



**Fig. S31.** MALDI analysis (PNA matrix, D<sub>2</sub>O, pD 7.2 phosphate buffer) of **CA** (0.1 mM) in the presence of 0.5 eq. **A8**.

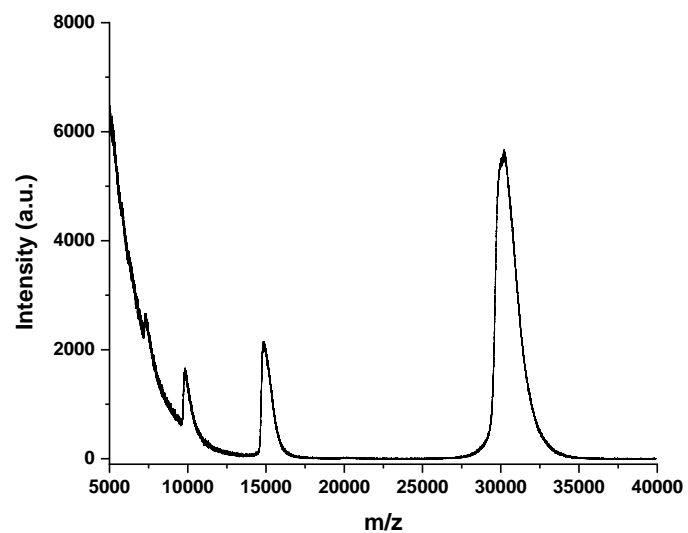


**Fig. S32.** MALDI analysis (PNA matrix, D<sub>2</sub>O, pD 7.2 phosphate buffer) of **CA** (0.1 mM) in the presence of 1 eq. **A8**.

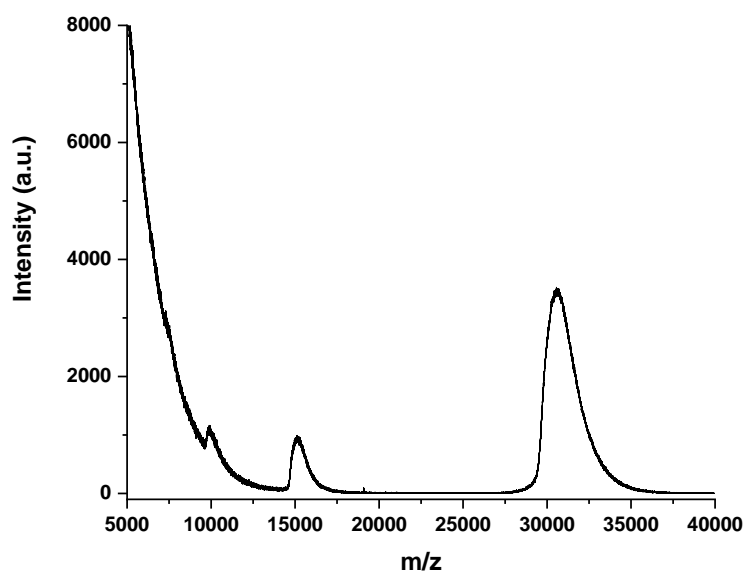


**Fig. S33.** MALDI analysis (PNA matrix, D<sub>2</sub>O, pD 7.2 phosphate buffer) of **CA** (0.1 mM) in the presence of 5 eq. **A8**.



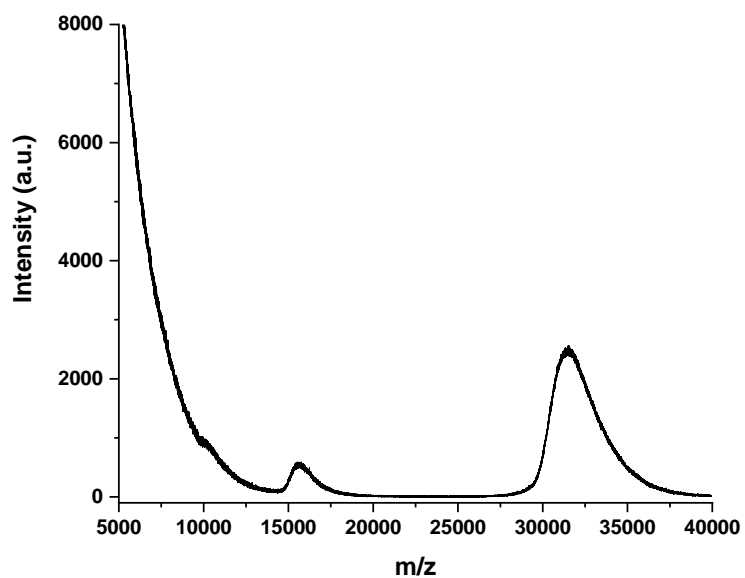


**Fig. S34.** MALDI analysis (PNA matrix, D<sub>2</sub>O, pD 7.2 phosphate buffer) of CA (0.1 mM) in the presence of 10 eq. A8.

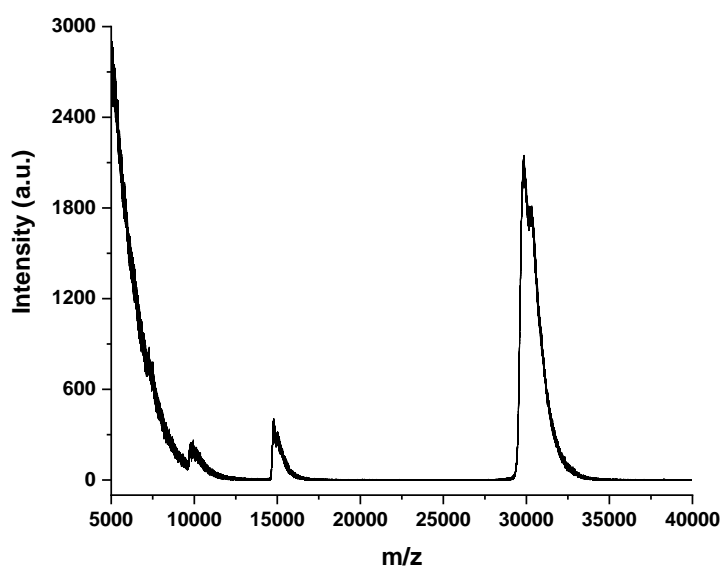


**Fig. S35.** MALDI analysis (PNA matrix, D<sub>2</sub>O, pD 7.2 phosphate buffer) of CA (0.1 mM) in the presence of 10 eq. A8 and 50 eq. H1.

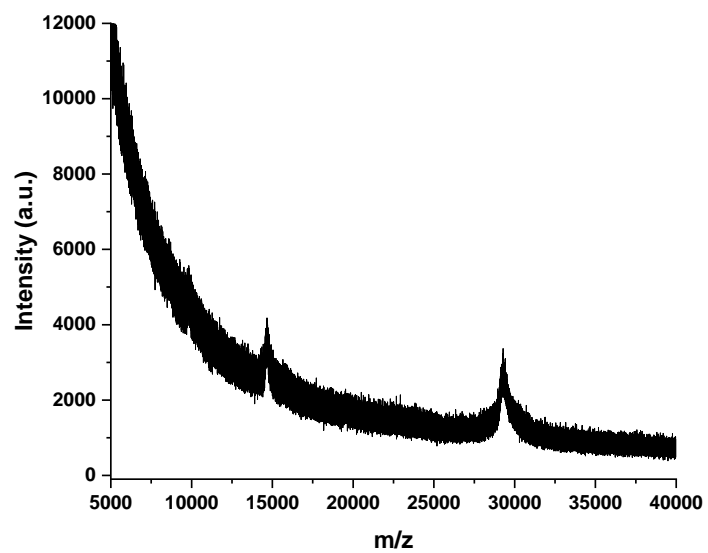


**Fig. S36.** MALDI analysis (PNA matrix, D<sub>2</sub>O, pD 7.2 phosphate buffer) of CA (0.1 mM) in the absence of A7.

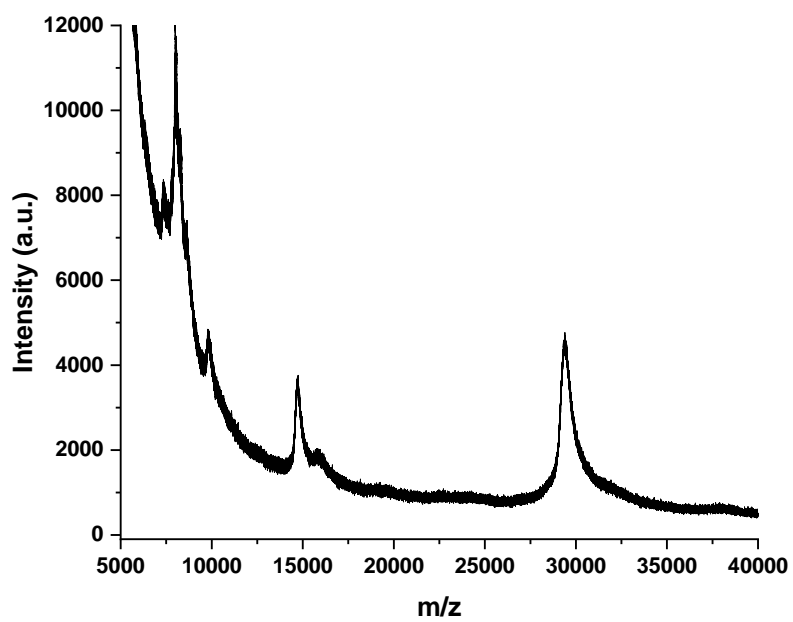


**Fig. S37.** MALDI analysis (PNA matrix, D<sub>2</sub>O, pD 7.2 phosphate buffer) of CA (0.1 mM) in the presence of 0.5 eq. A7.

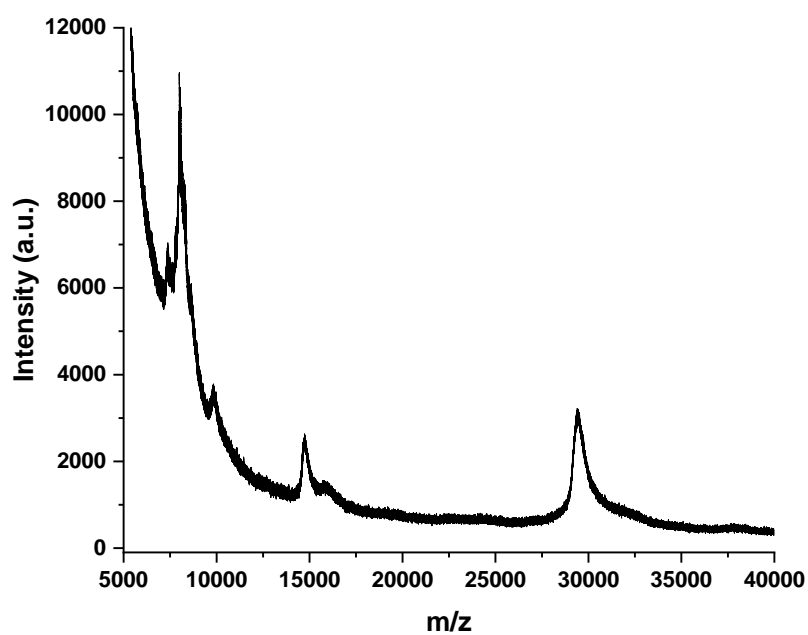


**Fig. S38.** MALDI analysis (PNA matrix, D<sub>2</sub>O, pH 7.2 phosphate buffer) of **CA** (0.1 mM) in the presence of 1 eq. **A7**.

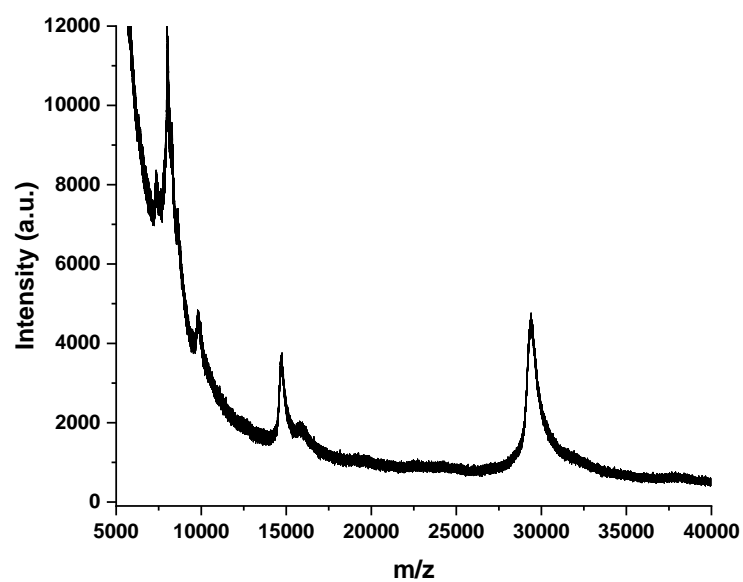


**Fig. S39.** MALDI analysis (PNA matrix, D<sub>2</sub>O, pH 7.2 phosphate buffer) of **CA** (0.1 mM) in the presence of 5 eq. **A7**.

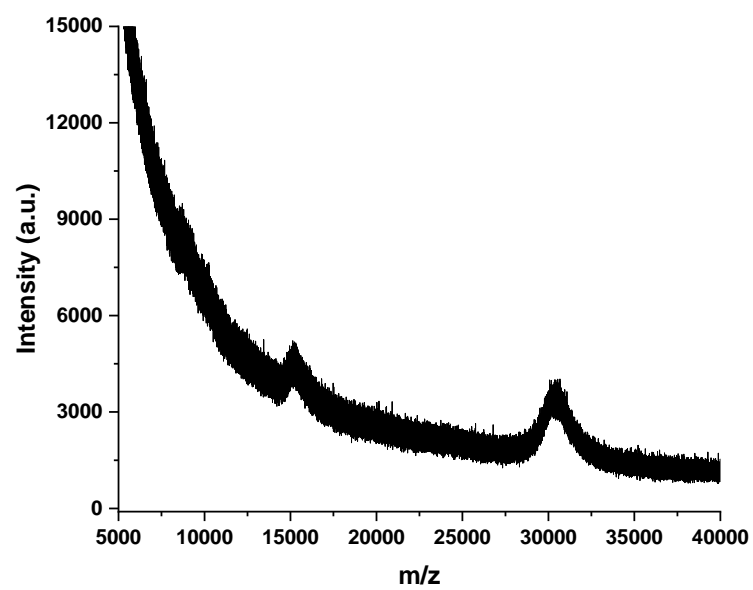


**Fig. S40.** MALDI analysis (PNA matrix, D<sub>2</sub>O, pD 7.2 phosphate buffer) of CA (0.1 mM) in the presence of 10 eq. **A7**.

## 5. DFT cartesian coordinates and energies

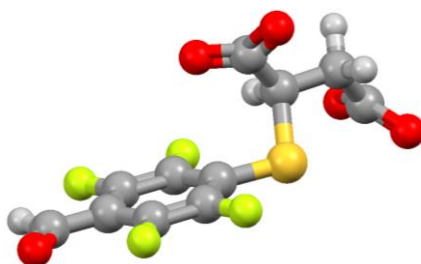
- Lowest energy conformation for  $\text{H}_3\text{O}^+$ .



**Cartesian coordinates (4 atoms), E (298.15 K) = -76.837952 Hartree**

1	H	-5.2207	-0.5771	0
2	H	-5.2207	0.8154	0.8044
3	H	-5.2207	0.8154	-0.8044
4	O	-5.5279	0.3513	0

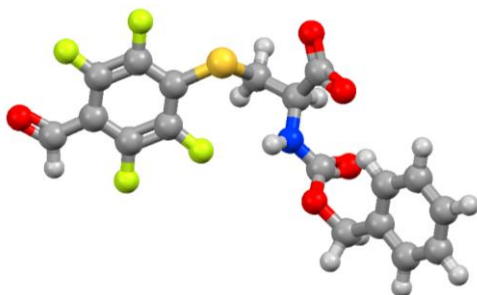
- Lowest energy conformation for  $\text{A7}^{2-}$ .



**Cartesian coordinates (25 atoms), E (298.15 K) = -1595.801763 Hartree**

1	C	0.9259	2.5797	-1.5674
2	C	1.18	1.4039	-0.8812
3	C	0.2585	0.8544	0.0162
4	C	-0.9321	1.5619	0.2081
5	C	-1.1936	2.7254	-0.4874
6	C	-0.2763	3.2766	-1.3935
7	C	-0.6062	4.5312	-2.1011
8	O	0.1151	5.0963	-2.8968
9	S	0.6537	-0.6348	0.8851
10	C	-0.8672	-1.7065	0.5896
11	C	-1.1187	-1.7861	-0.95
12	C	-0.5987	-3.0327	1.2904
13	C	-0.4499	-2.8772	2.8278
14	O	0.667	-3.1772	3.322
15	O	-1.4624	-2.4438	3.4349
16	O	-0.6251	-2.7617	-1.5595
17	O	-1.7928	-0.8368	-1.4207
18	F	1.8614	3.0232	-2.4161
19	F	-2.3652	3.3499	-0.2656
20	F	-1.8457	1.1296	1.0887
21	F	2.3487	0.7801	-1.1109
22	H	-1.599	4.9383	-1.8458
23	H	-1.6951	-1.1978	1.0757
24	H	-1.4706	-3.6641	1.0857
25	H	0.2739	-3.5214	0.8548

- Lowest energy conformation for **A8**:

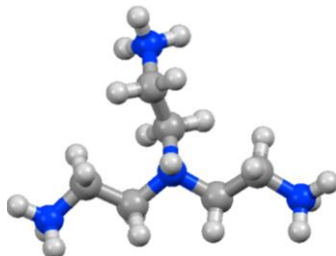


Cartesian coordinates (41 atoms), E (298.15 K) = -1921.974968 Hartree

1	C	-1.4373	3.5527	-4.3547
2	C	-0.7879	2.3306	-4.4147
3	C	-1.0473	1.3063	-3.4956
4	C	-1.9827	1.5852	-2.4945
5	C	-2.6448	2.7984	-2.4434
6	C	-2.3913	3.8218	-3.3652
7	F	-1.1325	4.4662	-5.2817
8	F	-3.5358	2.9937	-1.4576
9	F	0.1083	2.1403	-5.3961
10	F	-2.2539	0.6705	-1.5497
11	C	-3.1163	5.1084	-3.2538
12	S	-0.112	-0.1996	-3.5999
13	O	-2.9661	6.0572	-3.993
14	C	-1.4064	-1.5354	-3.4255
15	C	-1.0315	-2.5535	-2.3554
16	N	-1.2457	-2.0423	-1.0108
17	C	0.425	-3.1295	-2.5458
18	C	-1.6226	-2.8769	-0.014
19	O	0.9781	-3.5875	-1.5233
20	O	0.865	-3.0825	-3.7195
21	O	-1.3169	-2.3216	1.1974
22	O	-2.1827	-3.9503	-0.1454
23	C	-1.5509	-3.135	2.3567
24	C	-0.3513	-3.9865	2.7234
25	C	0.6781	-4.2471	1.8157
26	C	1.75	-5.0606	2.1898
27	C	1.8062	-5.619	3.4659
28	C	0.7789	-5.3598	4.3745
29	C	-0.2911	-4.5475	4.0043
30	H	-3.8316	5.1461	-2.4153
31	H	-2.3654	-1.0681	-3.2168
32	H	-1.4329	-2.0228	-4.396
33	H	-1.713	-3.4008	-2.4725
34	H	-0.6576	-1.2708	-0.7287
35	H	-1.7837	-2.4342	3.1607
36	H	-2.4238	-3.7697	2.1822
37	H	0.6569	-3.8281	0.8156

38	H	2.5426	-5.2565	1.4756
39	H	2.6424	-6.248	3.7527
40	H	0.8137	-5.785	5.372
41	H	-1.0846	-4.345	4.7174

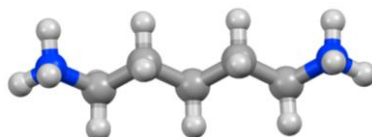
- Lowest energy conformation for  $T^{4+}$ .



**Cartesian coordinates (32 atoms), E (298.15 K) = -460.109097 Hartree**

1	C	-0.6895	-1.1699	0.6158
2	C	-2.1237	-1.1889	1.1462
3	N	-2.4537	-2.5705	1.6356
4	N	-0.2477	0.2227	0.1946
5	C	1.2321	0.1782	-0.1648
6	C	1.8427	1.5809	-0.1702
7	N	3.3052	1.4981	-0.4999
8	C	-1.0921	0.8062	-0.9389
9	C	-2.1014	1.8331	-0.4179
10	N	-2.9251	2.3618	-1.5566
11	H	-2.411	-3.2717	0.8893
12	H	-3.4903	1.6325	-2.0019
13	H	3.8203	0.899	0.1517
14	H	-3.407	-2.5909	2.0095
15	H	-3.5757	3.077	-1.2167
16	H	3.7305	2.429	-0.4467
17	H	-0.332	0.8212	1.0225
18	H	-1.8313	-2.8785	2.3891
19	H	-2.3539	2.8032	-2.2842
20	H	3.4749	1.1477	-1.4477
21	H	-0.5664	-1.8151	-0.2536
22	H	0.0025	-1.4855	1.395
23	H	-2.2489	-0.5201	1.9966
24	H	-2.861	-0.9537	0.3824
25	H	1.717	-0.4403	0.5888
26	H	1.3061	-0.3178	-1.1315
27	H	1.3958	2.2391	-0.9117
28	H	1.7655	2.0495	0.8099
29	H	-1.574	-0.0287	-1.4445
30	H	-0.4141	1.2689	-1.6511
31	H	-1.6061	2.6901	0.0357
32	H	-2.8012	1.4114	0.2999

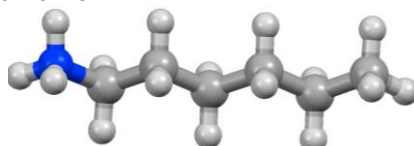
- Lowest energy conformation for **B2<sup>2+</sup>**.



**Cartesian coordinates (23 atoms), E (298.15 K) = -309.298098 Hartree**

1	C	-2.5316	-0.225	-0.0235
2	C	-1.2124	0.534	-0.0008
3	C	-0.0254	-0.4363	0.0026
4	C	1.3178	0.3027	-0.009
5	C	2.4767	-0.6837	0.0212
6	N	3.8057	0.0353	-0.0067
7	N	-3.7062	0.7251	0.0154
8	H	-2.6449	-0.816	-0.9316
9	H	-2.6395	-0.8809	0.8396
10	H	-1.1689	1.1702	0.8892
11	H	-1.1515	1.1894	-0.8759
12	H	-0.0865	-1.0938	-0.871
13	H	-0.0823	-1.0779	0.8883
14	H	1.38	0.9699	0.857
15	H	1.3875	0.9254	-0.907
16	H	2.4689	-1.3463	-0.8435
17	H	2.473	-1.2878	0.9278
18	H	4.5858	-0.6255	0.0146
19	H	3.9119	0.6602	0.7963
20	H	3.9086	0.602	-0.8522
21	H	-4.5952	0.2215	-0.0272
22	H	-3.7105	1.281	0.8741
23	H	-3.6881	1.3796	-0.7707

- Lowest energy conformation for **B3<sup>+</sup>**.



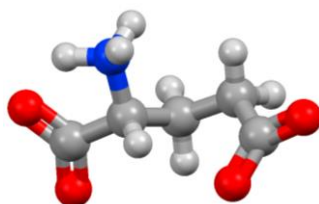
**Cartesian coordinates (23 atoms), E (298.15 K) = -292.806275 Hartree**

1	C	-2.5936	-0.2443	-0.0207
2	C	-1.2719	0.5089	0.0047
3	C	-0.0823	-0.4588	0.0061
4	C	1.267	0.2661	-0.0044
5	C	2.4629	-0.6911	0.0177
6	C	3.8095	0.0371	-0.0101
7	N	-3.7668	0.7099	0.0094
8	H	-2.7058	-0.8382	-0.9272
9	H	-2.7081	-0.8969	0.8442
10	H	-1.2286	1.1445	0.8959
11	H	-1.2101	1.1676	-0.8684
12	H	-0.1471	-1.1173	-0.8681
13	H	-0.1421	-1.1054	0.8895



14	H	1.3251	0.9387	0.8605
15	H	1.3286	0.9032	-0.8955
16	H	2.3955	-1.3713	-0.8398
17	H	2.4034	-1.3202	0.914
18	H	4.6453	-0.6677	0.0111
19	H	3.9127	0.7045	0.8514
20	H	3.9077	0.6455	-0.9147
21	H	-4.6581	0.2108	-0.0334
22	H	-3.7704	1.2707	0.8649
23	H	-3.7417	1.3602	-0.7799

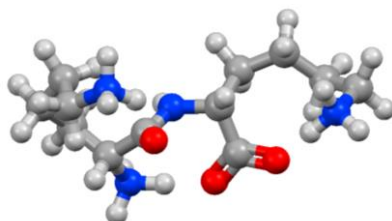
- Lowest energy conformation for **B4**:



**Cartesian coordinates (18 atoms), E (298.15 K) = -551.240975 Hartree**

1	N	-1.8498	0.1635	-0.8359
2	C	-0.517	0.7872	-0.4769
3	C	-0.8331	2.2976	-0.2318
4	C	0.15	0.0922	0.7035
5	O	0.1059	3.0036	0.1621
6	O	-2.0297	2.632	-0.4806
7	C	0.5372	-1.3635	0.4347
8	C	1.5994	-1.5882	-0.6823
9	O	1.8329	-2.7883	-0.9621
10	O	2.1315	-0.5676	-1.1926
11	H	-1.8477	-0.336	-1.7223
12	H	-2.2063	-0.4604	-0.1133
13	H	-2.4495	1.0375	-0.8816
14	H	0.1369	0.6932	-1.3429
15	H	1.0449	0.6758	0.9181
16	H	-0.5035	0.1659	1.5826
17	H	0.9384	-1.8059	1.3531
18	H	-0.3388	-1.9741	0.1845

- Lowest energy conformation for **KK<sup>+</sup>**:

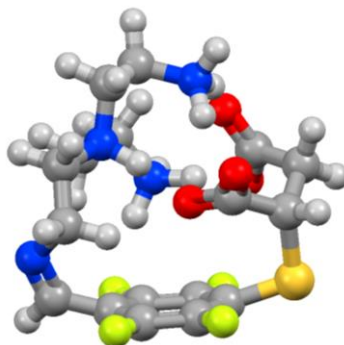


**Cartesian coordinates (47 atoms), E (298.15 K) = -918.511927 Hartree**

1	N	-0.9536	-1.2815	2.5909
2	C	-1.6048	-0.0988	1.8846
3	C	-0.6304	0.2977	0.7642

4	C	-3.0313	-0.4459	1.4379
5	O	-0.1174	1.4148	0.7452
6	C	-3.906	0.7538	1.0294
7	C	-3.3404	1.6496	-0.0973
8	C	-2.6891	2.9271	0.4482
9	N	-1.6088	3.4294	-0.4756
10	N	-0.3204	-0.6735	-0.1207
11	C	1.0465	-0.7527	-0.65
12	C	2.0249	-0.9968	0.5474
13	C	1.0778	-1.8364	-1.7505
14	O	3.2487	-0.8158	0.3321
15	O	1.5439	-1.3556	1.6529
16	C	2.2395	-1.7626	-2.756
17	C	3.5754	-2.3947	-2.2934
18	C	4.8026	-1.5183	-2.5248
19	N	4.6647	-0.2012	-1.794
20	H	-0.9825	-1.1613	3.6035
21	H	-1.432	-2.1596	2.3833
22	H	0.0716	-1.3778	2.2725
23	H	-1.6078	0.7207	2.5997
24	H	-2.9875	-1.165	0.6134
25	H	-3.5257	-0.953	2.2712
26	H	-4.8653	0.3432	0.7101
27	H	-4.1198	1.3616	1.9143
28	H	-2.623	1.0836	-0.6996
29	H	-4.1407	1.9333	-0.7829
30	H	-3.4179	3.7265	0.5682
31	H	-2.1912	2.7649	1.4013
32	H	-1.281	4.3574	-0.2015
33	H	-0.8062	2.7834	-0.4132
34	H	-1.9232	3.4861	-1.446
35	H	-0.786	-1.5657	-0.0203
36	H	1.2942	0.2167	-1.0838
37	H	1.0397	-2.829	-1.288
38	H	0.1465	-1.718	-2.3111
39	H	1.9167	-2.2647	-3.6705
40	H	2.3742	-0.7148	-3.0454
41	H	3.5318	-2.6481	-1.234
42	H	3.7496	-3.3307	-2.8289
43	H	5.6974	-2.0019	-2.136
44	H	4.9602	-1.2963	-3.58
45	H	5.574	0.1797	-1.5357
46	H	4.2021	0.5026	-2.3676
47	H	4.0736	-0.3489	-0.9101

- Lowest energy conformation for A7T\*.

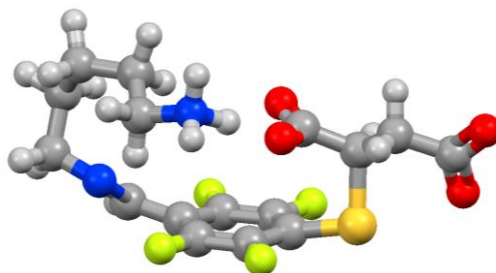


Cartesian coordinates (53 atoms), E (298.15 K) = -1979.133369 Hartree

1	C	1.6535	3.2178	-1.4843
2	C	-0.5315	3.7726	-0.6406
3	C	0.0851	4.1564	0.5504
4	C	1.4485	3.9986	0.7401
5	C	2.2462	3.4346	-0.2465
6	C	3.5824	2.8186	0.0173
7	F	2.3966	2.6603	-2.4779
8	F	-0.6532	4.5395	1.6012
9	F	1.9717	4.2619	1.9516
10	S	-2.2941	3.5662	-0.7211
11	C	-2.5808	1.9772	0.2608
12	C	-3.0317	0.7825	-0.626
13	C	-1.4428	1.457	1.1671
14	O	-0.3069	1.2889	0.6466
15	O	-1.7887	1.0861	2.3125
16	C	-1.863	0.0611	-1.2963
17	O	-1.4013	0.6009	-2.3409
18	O	-1.4009	-0.9944	-0.7816
19	C	0.2973	3.3886	-1.6941
20	F	-0.1987	3.0718	-2.8936
21	N	3.789	1.8572	0.8228
22	C	2.7348	1.3612	1.7069
23	C	2.5323	-0.1507	1.6423
24	N	1.5968	-0.6305	0.5366
25	C	2.3397	-0.6404	-0.7868
26	C	1.5908	-1.1131	-2.0383
27	C	1.0806	-2.0166	0.8576
28	C	0.1523	-2.1425	2.0585
29	N	-1.1853	-1.5052	1.8476
30	H	4.4118	3.1448	-0.6078
31	H	-3.4153	2.2564	0.9002
32	H	-3.56	0.0827	0.0261
33	H	-3.7266	1.1347	-1.3895
34	H	3.0799	1.5688	2.7237
35	H	1.7609	1.8386	1.5921
36	H	3.4743	-0.6866	1.5267
37	H	2.0741	-0.4556	2.5782

38	H	0.7867	0.05	0.5055
39	H	2.7425	0.3594	-0.9292
40	H	3.1877	-1.3062	-0.6316
41	H	2.3164	-1.6444	-2.6515
42	H	0.7725	-1.7924	-1.815
43	H	0.5584	-2.3801	-0.021
44	H	1.9547	-2.6456	1.0288
45	H	-0.0034	-3.2109	2.2009
46	H	0.5758	-1.7507	2.9805
47	H	-1.2507	-0.5294	2.2358
48	H	-1.4221	-1.4063	0.8173
49	H	-1.9178	-2.0499	2.3004
50	H	-0.0662	0.2459	-2.5889
51	H	1.588	0.8158	-2.8862
52	H	0.9446	-0.3375	-3.8398
53	N	1.0039	-0.0202	-2.8722

- Lowest energy conformation for **A7B2**:

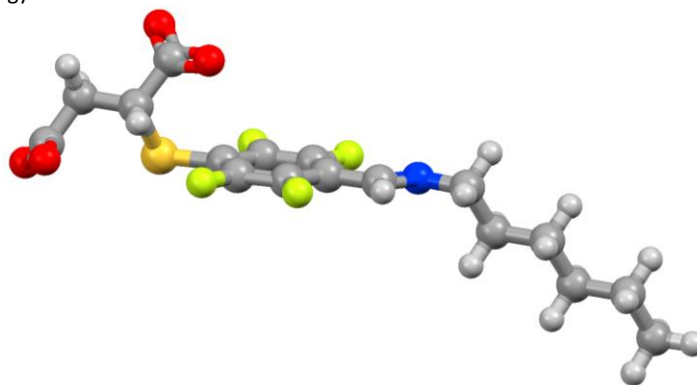


Cartesian coordinates (44 atoms), E (298.15 K) = -1828.231057 Hartree

1	C	-0.5898	1.4461	2.3716
2	C	0.1579	0.3091	2.6268
3	C	-0.3794	-0.9679	2.4618
4	C	-1.7341	-1.0479	2.1456
5	C	-2.4866	0.0901	1.9125
6	C	-1.9218	1.364	1.9587
7	C	-2.675	2.4928	1.3795
8	N	-2.0662	3.3938	0.7288
9	S	0.6509	-2.4297	2.4425
10	C	0.7825	-2.6146	0.5592
11	C	0.518	-1.2579	-0.1463
12	C	2.1509	-3.1805	0.1926
13	C	2.5435	-4.5451	0.8156
14	O	1.8997	-4.9187	1.8322
15	O	3.4936	-5.1414	0.2576
16	O	1.4419	-0.3878	-0.0218
17	O	-0.5457	-1.124	-0.7697
18	F	0.0242	2.6393	2.4762
19	F	-3.7706	-0.0523	1.5227
20	F	-2.3213	-2.2417	1.9619
21	F	1.4452	0.47	2.9666
22	C	-2.8467	4.3268	-0.0626

23	C	-2.8699	3.868	-1.5335
24	C	-1.5262	3.8159	-2.2825
25	C	-0.5555	2.6501	-1.9639
26	C	0.5415	3.0181	-0.9668
27	N	1.6389	1.9944	-0.9506
28	H	-3.7677	2.4305	1.4374
29	H	-0.013	-3.3034	0.2795
30	H	2.1904	-3.2877	-0.8973
31	H	2.9177	-2.445	0.4537
32	H	-3.8826	4.4128	0.2978
33	H	-2.3771	5.313	0.0034
34	H	-3.3513	2.8844	-1.5791
35	H	-3.5273	4.5621	-2.0677
36	H	-1.7693	3.7534	-3.347
37	H	-1.0057	4.7729	-2.1565
38	H	-1.1001	1.773	-1.6029
39	H	-0.0718	2.3509	-2.9007
40	H	0.9976	3.9721	-1.2391
41	H	0.1457	3.0965	0.0426
42	H	2.0482	1.8891	-1.8794
43	H	2.3924	2.3021	-0.3358
44	H	1.37	0.9752	-0.5937

- Lowest energy conformation for **A7B3<sup>-2</sup>**.

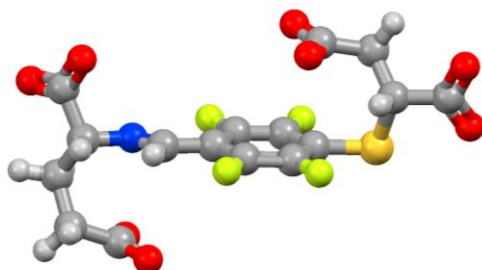


Cartesian coordinates (44 atoms), E (298.15 K) = -1811.711591 Hartree

1	C	0.5491	-1.7566	-0.7936
2	C	0.9988	-2.9267	-0.1984
3	C	0.3022	-3.5506	0.8377
4	C	-0.8775	-2.931	1.2524
5	C	-1.3352	-1.775	0.6498
6	C	-0.6404	-1.1391	-0.3886
7	C	-1.1874	0.1018	-0.9588
8	N	-0.6328	0.7568	-1.896
9	S	0.9305	-5.0248	1.5961
10	C	-0.515	-6.2156	1.3978
11	C	-0.9098	-6.2666	-0.111
12	C	-0.0768	-7.539	2.0139

13	C	0.1697	-7.4368	3.5433
14	O	1.335	-7.6775	3.9513
15	O	-0.8269	-7.1047	4.2351
16	O	-0.3659	-7.1487	-0.8149
17	O	-1.7386	-5.393	-0.4676
18	F	1.2943	-1.2441	-1.7839
19	F	-2.4895	-1.2415	1.1015
20	F	-1.5981	-3.4484	2.2605
21	F	2.1435	-3.4625	-0.661
22	C	-1.2864	1.9808	-2.3365
23	C	-0.3623	3.1876	-2.1331
24	C	-0.9618	4.4888	-2.6735
25	C	-0.0437	5.6988	-2.4749
26	C	-0.6326	7.0057	-3.0157
27	C	0.2954	8.2074	-2.8158
28	H	-2.13	0.4296	-0.5056
29	H	-1.3301	-5.795	1.9816
30	H	-0.9014	-8.2403	1.8425
31	H	0.7999	-7.9278	1.4931
32	H	-1.4983	1.8737	-3.407
33	H	-2.2457	2.1512	-1.8222
34	H	-0.1508	3.2932	-1.0626
35	H	0.5954	2.9848	-2.6249
36	H	-1.1798	4.3709	-3.7425
37	H	-1.9241	4.6801	-2.1822
38	H	0.1751	5.8162	-1.4057
39	H	0.9193	5.5064	-2.9653
40	H	-0.8535	6.8859	-4.0833
41	H	-1.5937	7.1982	-2.5237
42	H	-0.1486	9.1269	-3.2076
43	H	0.5091	8.3652	-1.7538
44	H	1.2514	8.0537	-3.3265

- Lowest energy conformation for **A7B4**<sup>-4</sup>.

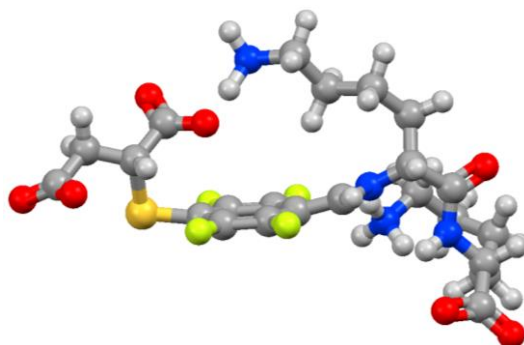


Cartesian coordinates (39 atoms), E (298.15 K) = -2070.120657999 Hartree

1	C	0.6457	-0.1295	-0.6324
2	C	0.7973	-1.5079	-0.6486
3	C	-0.2219	-2.373	-0.2544
4	C	-1.4126	-1.7777	0.1586
5	C	-1.5609	-0.4047	0.1904

6	C	-0.5434	0.4731	-0.2057
7	C	-0.7939	1.9217	-0.1593
8	S	-0.0133	-4.1466	-0.2759
9	C	0.0083	-4.5152	1.5573
10	C	0.0163	-6.0666	1.7072
11	C	1.1639	-3.8352	2.2887
12	C	0.9499	-2.3261	2.5937
13	O	-0.1923	-2.0046	3.0121
14	O	1.9389	-1.5703	2.4248
15	O	-0.0329	-6.4702	2.8914
16	O	0.0683	-6.7553	0.6581
17	F	1.7005	0.6092	-1.0177
18	F	-2.7412	0.0955	0.6215
19	F	-2.4459	-2.539	0.5614
20	F	1.9865	-1.9995	-1.0437
21	N	0.0211	2.7958	-0.5881
22	C	-0.3666	4.1896	-0.4834
23	C	0.598	4.8696	0.5713
24	C	-0.3546	4.8489	-1.8661
25	O	0.498	4.4096	1.7329
26	O	1.3452	5.7894	0.166
27	C	-1.479	4.3603	-2.7914
28	C	-1.2647	2.9368	-3.376
29	O	-2.1868	2.0979	-3.2028
30	O	-0.187	2.7553	-4.0008
31	H	-1.7684	2.1999	0.2542
32	H	-0.9229	-4.1269	1.9728
33	H	1.2396	-4.3463	3.2553
34	H	2.1066	-3.9839	1.7561
35	H	-1.3823	4.2789	-0.0572
36	H	-0.4286	5.9285	-1.7075
37	H	0.6092	4.6625	-2.3459
38	H	-2.4412	4.3977	-2.2695
39	H	-1.5458	5.0457	-3.6464

- Lowest energy conformation for **A7KK**.



Cartesian coordinates (68 atoms), E (298.15 K) = -2437.447269 Hartree

1	C	1.1432	0.5719	2.1565
2	C	1.8628	-0.4822	2.6904

3	C	1.2367	-1.504	3.403
4	C	-0.1343	-1.3777	3.623
5	C	-0.8532	-0.3282	3.0836
6	C	-0.2463	0.6653	2.3028
7	C	-1.1062	1.572	1.5412
8	S	2.1187	-2.9785	3.8466
9	C	1.2395	-4.1933	2.703
10	C	1.337	-3.6669	1.258
11	C	1.8627	-5.5607	2.9387
12	C	1.5368	-6.1421	4.3464
13	O	0.3297	-6.0873	4.6927
14	O	2.5005	-6.6197	4.9926
15	O	2.2562	-4.0343	0.5181
16	O	0.4043	-2.8393	0.9377
17	F	1.8233	1.4629	1.4114
18	F	-2.184	-0.3021	3.2714
19	F	-0.8004	-2.3251	4.2977
20	F	3.1769	-0.5403	2.4339
21	N	-0.6719	2.4467	0.7209
22	C	-1.6352	3.0584	-0.1881
23	C	-1.5562	4.603	-0.1226
24	C	-1.3647	2.5569	-1.6198
25	O	-1.6924	5.2916	-1.1289
26	C	-1.5141	1.0371	-1.8192
27	C	-0.2619	0.1973	-1.5132
28	C	-0.453	-1.255	-1.9423
29	N	0.6823	-2.112	-1.4799
30	N	-1.2982	5.1035	1.1093
31	C	-1.4076	6.5224	1.4602
32	C	-2.0359	6.6099	2.894
33	C	-0.0564	7.2613	1.4419
34	O	-2.3004	7.7619	3.2932
35	O	-2.1861	5.5174	3.5015
36	C	0.6538	7.3693	0.0668
37	C	1.9376	6.5394	-0.1391
38	C	1.7516	5.0379	-0.3517
39	N	1.5027	4.2902	0.9342
40	H	-2.1761	1.3733	1.6397
41	H	0.2019	-4.2086	3.0281
42	H	1.4287	-6.2348	2.1912
43	H	2.9397	-5.5381	2.7641
44	H	-2.6652	2.787	0.0914
45	H	-2.0682	3.0838	-2.266
46	H	-0.3643	2.8775	-1.9273
47	H	-2.3571	0.6654	-1.2247
48	H	-1.7863	0.8657	-2.8658
49	H	0.5984	0.6196	-2.0446
50	H	-0.0162	0.2234	-0.4516



51	H	-1.3597	-1.6763	-1.5032
52	H	-0.5357	-1.3289	-3.0281
53	H	0.7128	-2.991	-1.9947
54	H	1.5808	-1.6553	-1.6324
55	H	0.5882	-2.4074	-0.3646
56	H	-1.5102	4.5313	1.9306
57	H	-2.0825	7.0086	0.7513
58	H	0.6089	6.8112	2.1912
59	H	-0.2713	8.2618	1.8199
60	H	-0.0556	7.1238	-0.7278
61	H	0.9369	8.4141	-0.0862
62	H	2.4357	6.9073	-1.0406
63	H	2.641	6.71	0.6839
64	H	2.6336	4.5834	-0.7998
65	H	0.9	4.8425	-1.0018
66	H	2.3642	4.1286	1.4551
67	H	1.0126	3.3834	0.773
68	H	0.8507	4.8096	1.5257

## 6. References

1- M.J. A Frisch, G.W.Trucks, H.B. Schlegel, G.E. Scuseria, M.A. Robb, J.R. Cheeseman, G. Scalmani, V. Barone, B. Mennucci, G.A. Petersson, et al. Gaussian 09, Revision B.01 (Gaussian, Inc), **2010**.

2- A.D. Becke, *J. Chem. Phys.*, 1993, **98**, 5648–5652.

3- S. Miertus and J. Tomasi, *Chem. Phys.*, 1982, **65**, 239–241.

4- A. Grosdidier, V. Zoete and O. Michielin, *Nucleic Acids Res.*, 2011, **39**, W270-277.